

SURVEY OF I_E^{TM} CLUSTERS

S. Y. LO

*Originally published as Physical, Chemical and
Biological Properties of Stable Water Clusters,
Proceedings of the First International Symposium.
Reprinted here by permission of
World Scientific Publishing Company, 1998.*

Water clusters, referred to as I_E Crystals, that are stable at room temperature, have been discovered and studied recently. Three different sizes of I_E Crystals centering around 15nm, 300nm and 3 microns were identified by means of laser autocorrelation method.

The larger, micron size clusters were also detected by transmission electron microscopy (TEM). Additionally, three-dimensional structures of I_E Crystals were observed with atomic force microscopy (AFM). The electric dipole nature of I_E Crystals was demonstrated by crystallization of sodium phosphate solution under an external electric field.

Tile sodium phosphate crystals obtained from I_E -based solution were formed in a very regular manner, along the electric field lines, while a random crystallization was observed in the case of sodium phosphate solution prepared with a pure water control.

The measurements of resistivity and electromotive force of I_E solutions also indicated a presence of electric dipole potential. A detected shift of hydrogen peak position in nuclear magnetic resonance (NMR) spectra of I_E solutions suggested a changed arrangement of water molecules in I_E solutions as compared to regular water.

The possible applications of I_E Crystals and their solutions to physical, chemical, biochemical and medical processes are discussed.

1 Introduction

Water is one of the crucial components of life and its structure, unusual physical and chemical properties have been studied comprehensively. A number of models was proposed, based on the clustering of water molecules, to account for its negative volume of melting, density maximum at 4°C, and anomalous high melting and boiling temperatures¹⁻²¹. Negatively charged water clusters of eight or more molecules were observed by Armbruster¹⁸. Larger clusters with 50-100 water molecules were predicted by other research groups^{19,20}.

Advances in laser spectroscopy and theoretical dynamics allowed highly detailed studies of small water clusters and offered insights into hydrogen-bond network rearranging dynamics²¹. It has been established that at least 10 types of ice structures exist²³⁻²⁴. Stable rigid structures, such as ice VI and VII, are known to be formed by water molecules at room temperature and at pressure above 7 kilobars²² (Figure 1). A dissolved salt appears to cause an effect on water similar to that produced by high external pressure^{35,36}. Rigid associations of water molecules, called IE Crystals, were observed in specially prepared dilute aqueous solutions at room temperature and normal pressure^{36,37}.



In this study, we describe the structure of IE Crystals and demonstrate that their formation is governed by the large electric dipole moment of water molecules.

2 A Possible Mechanism of IE Crystal Formation in Aqueous Solutions

A new kind of stable water cluster³⁸, IE Crystal, formed by the electric dipole moment of water molecules has been proposed^{36,37}. We have discovered that IE Crystals can be created from a dilute aqueous solution, for example sodium chloride, by their repeated dilution and shaking until the desired result is achieved.

To better understand the interaction between electric dipole moments of water molecules, an analogy can be made with a magnet made of iron atoms. Each iron atom can be viewed as a small magnet with a North and a South pole. When the magnetic dipole moments of iron atoms align, a magnet is created with a large magnetic dipole moment equal to the sum of the individual dipole moments. Similarly, when permanent electric dipole moments of water molecules line up, a stable water cluster with a large electric dipole moment is formed (Table I).

Table 1 A comparison of an IE cluster formed from water molecules with a magnet made of iron atoms.

	 Water Molecules	 Fe Atom
Microscopic	Permanent electric dipole moment (nm)	Magnetic dipole moment (nm)
Macroscopic	Stable Water cluster(μm) 10^{10} molecules	Magnet(m)

The water molecules, in ordinary water are at their lowest energy state in a potential well. A computer modeling of the potential energy of the surface of water, suggests an existence of several local minima besides the lowest energy state (Figure 2a). A dipole moment D_0 presents the lowest (ground) stable state, and a larger dipole moment D_1 corresponds to a metastable state. The term "metastable" describes a stable, but not the lowest energy state. Its stability is due to a potential barrier that prevents molecules from falling back into the lowest stable state. The detailed mechanism is discussed in Wong and Lo³⁹.

The Phase Diagram of Ice

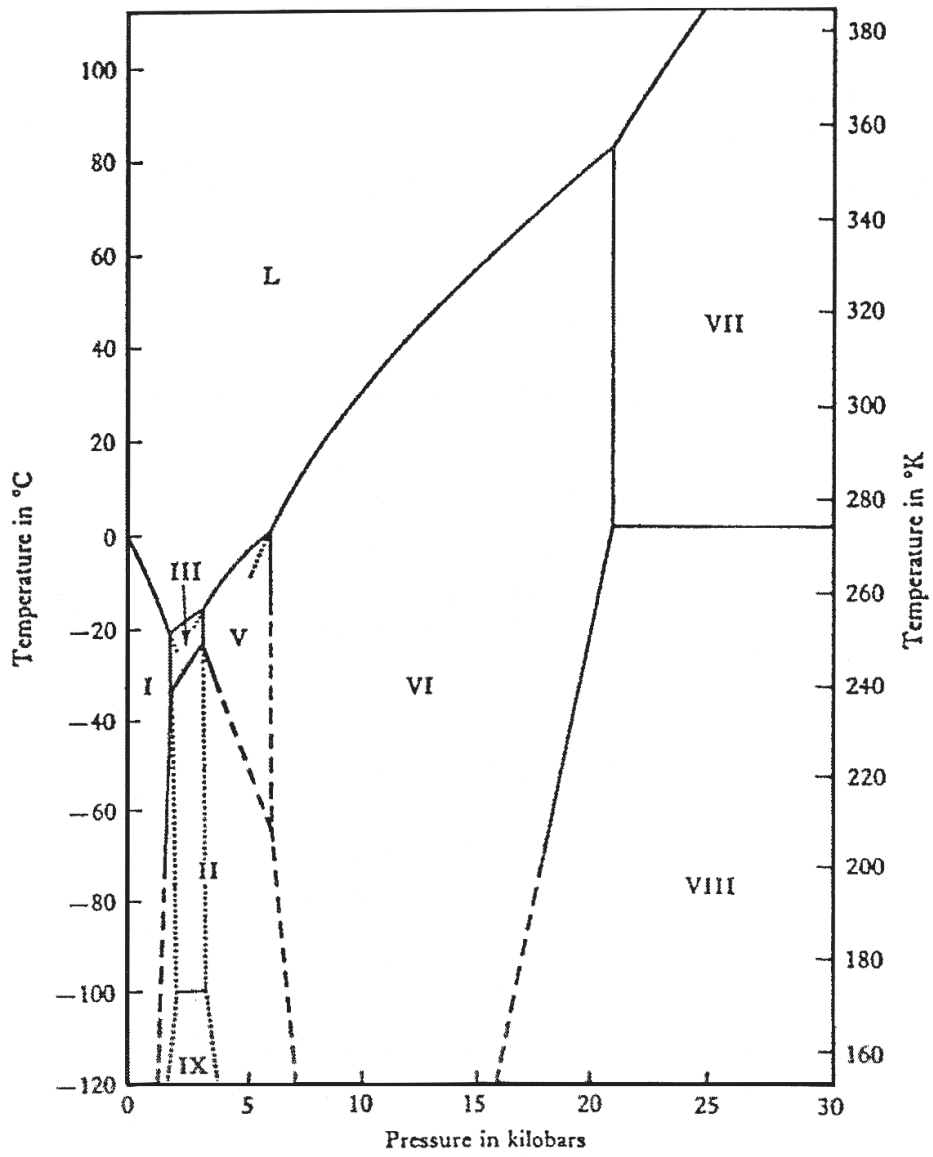
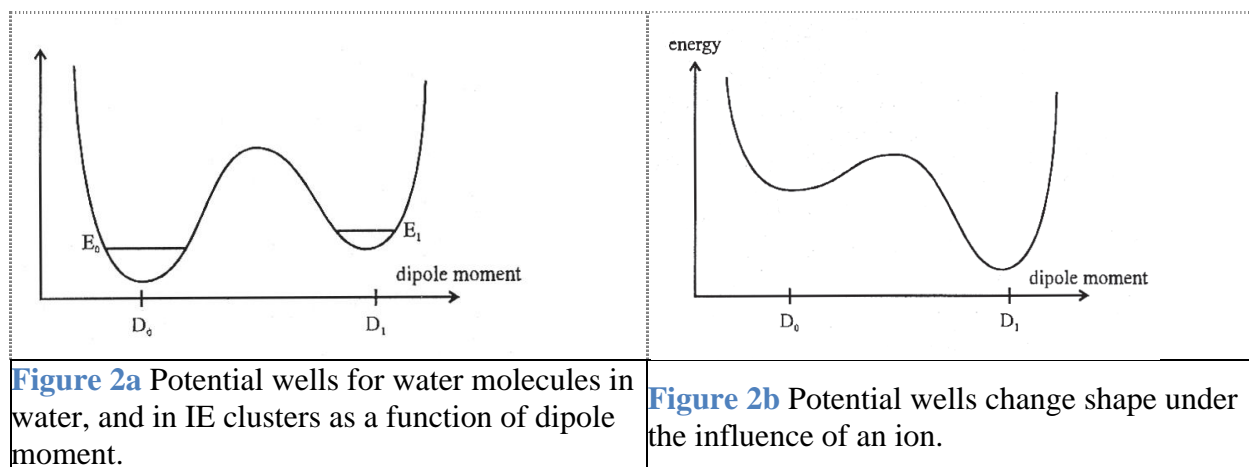


Figure 1 Phase diagram of ice based on temperature and pressure.

When a charged ion, e.g. Na^+ , is present in a dilute electrolyte solution, a local electric field around the ion is created. This electric field distorts the energy potential of local water molecules as shown in Figure 2b. As a result, the metastable state becomes lower in energy than the ground state, and the water molecules can then form easily into a larger dipole moment entity. A vigorous shaking of the solution results in a separation of charged ions from associations of water molecules. As a result, the shape of potential wells quickly restores and the ground state becomes the lowest energy state again. The restored potential barrier between metastable and ground states prevents the water clusters from sliding into the ground state.



3 Detection of I_E Clusters

Three methods were used to detect stable IE clusters: Photon Autocorrelation, Transmission Electron Microscopy (TEM) and Atomic Force Microscopy (AFM).

3.1 Size Distribution of I_E Clusters as Determined by Photon Autocorrelation

Photon Autocorrelation method, which utilizes the self-interference phenomenon of photons, was used to study the size distribution of I_E clusters. A helium-neon laser (Model BI-9000, Digital Correlation, Brookhaven Instruments Corporation) emitted light on a glass bottle containing an I_E Crystal aqueous solution. The interference between the light scattered by I_E Crystals and the transmitted light, allowed us to estimate the size of I_E : clusters (Figure 3). Three major sizes of I_E clusters were observed: approximately 15nm, 300nm and several microns (Figure 3a).

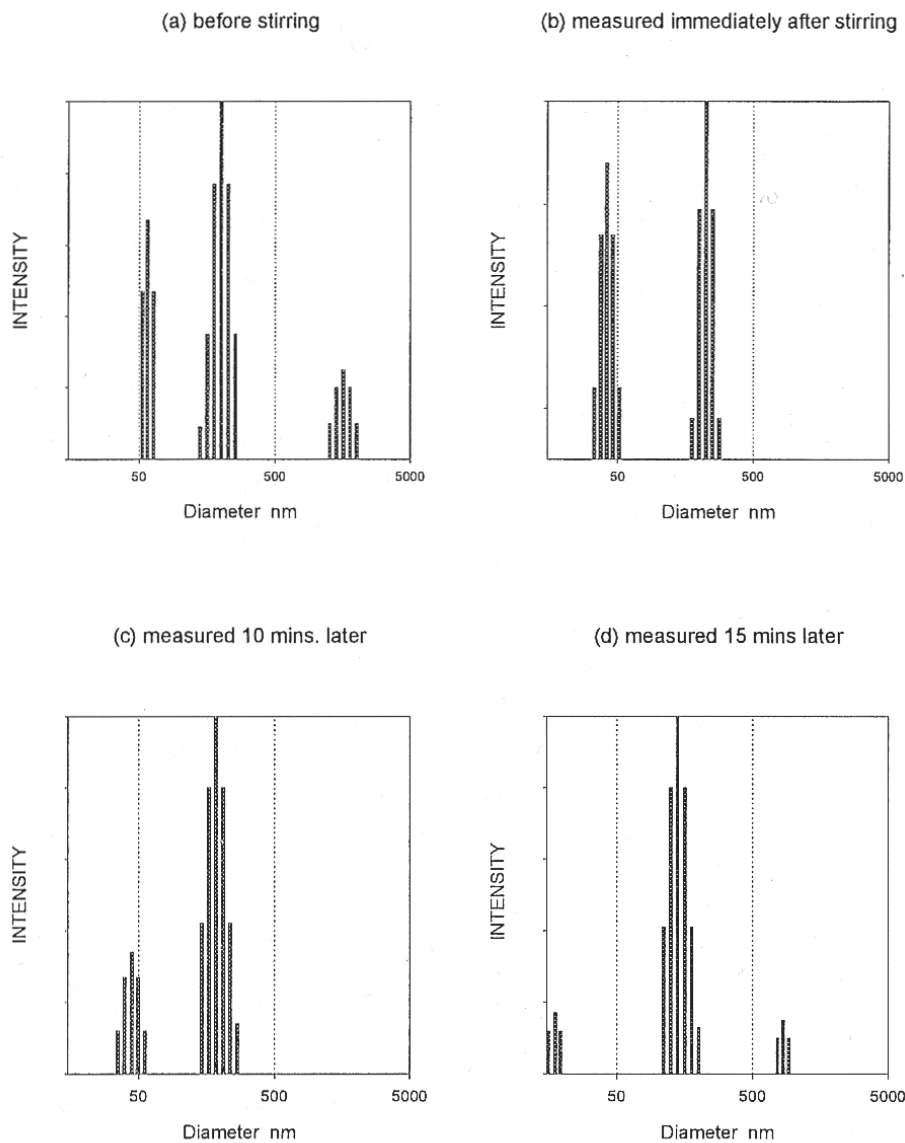


Figure 3 Size distribution of IE clusters as determined by in situ laser autocorrelation measurement.

Vigorous stirring of I_E Crystal solution led to the complete disappearance of the largest I_E clusters, while the number of smaller, 10nm and 100nm size, clusters increased (Figure 3b). This observation indicates that stirring (or shaking) breaks down large I_E clusters into the smaller ones. The smaller I_E clusters have strong electric dipole moments, which act like magnets to attract one to another to form larger I_E clusters. Approximately 15 minutes after stirring, many of the smaller I_E clusters reassembled back to their original larger size, and the solution became stable again (Figure 3d).

3.2 Observation of the Two-Dimensional Structure of I_E Crystals with TEM

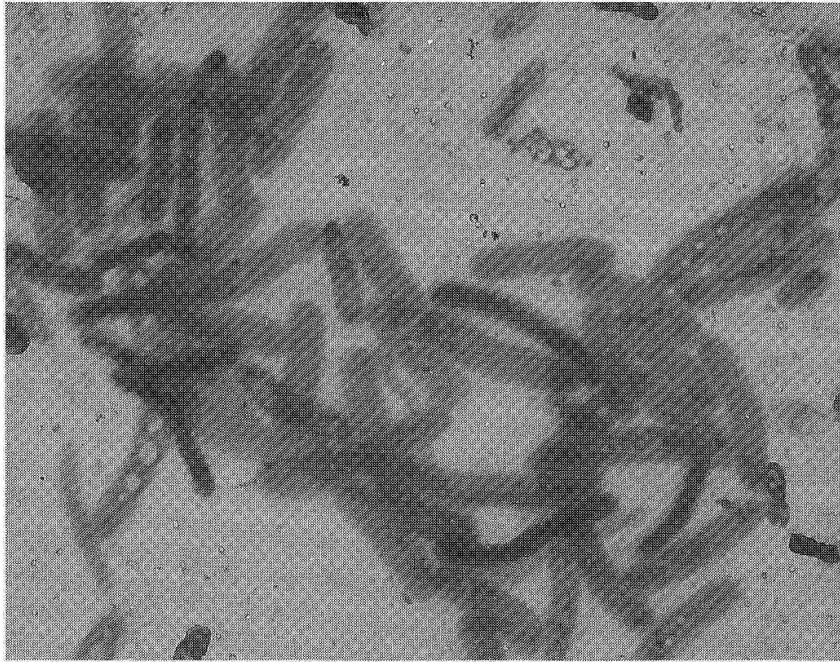
The following EPA approved method for Asbestos Fiber Analysis (EPA-600/4-83-043) was used to prepare I_E Crystal samples. About 25 ml of I_E solution was filtered through a 0.1 μm pore size Nucleopore filter. The filter was then coated with carbon in a vacuum evaporator. The obtained carbon coated filter was cut in small pieces and placed on top of an electron microscope copper grid. The assembly was then placed onto the chloroform-saturated lens tissue and incubated for 24 h. to partially dissolve the filter, The residual filter was dissolved in a chloroform condensation washer. This method allowed us to preserve particles, including I_E structures, under a carbon film and then to transfer them to a microscope grid with a minimum of particle movement and breakage of carbon film.

Various I_E Crystal solutions were prepared using ATG's proprietary technologies. The I_E Crystals were deposited on microscope grids (as described above), and were observed with a Hitachi H600A TEM. Different shapes of I_E clusters were noticed (Figure 4). Such a variation in I_E Crystal structure is not surprising, since quantum mechanical calculations of the potential energy surface of water clusters, suggest existence of many Local metastable energy minima. Theoretically, each of these minima can produce a different cluster.

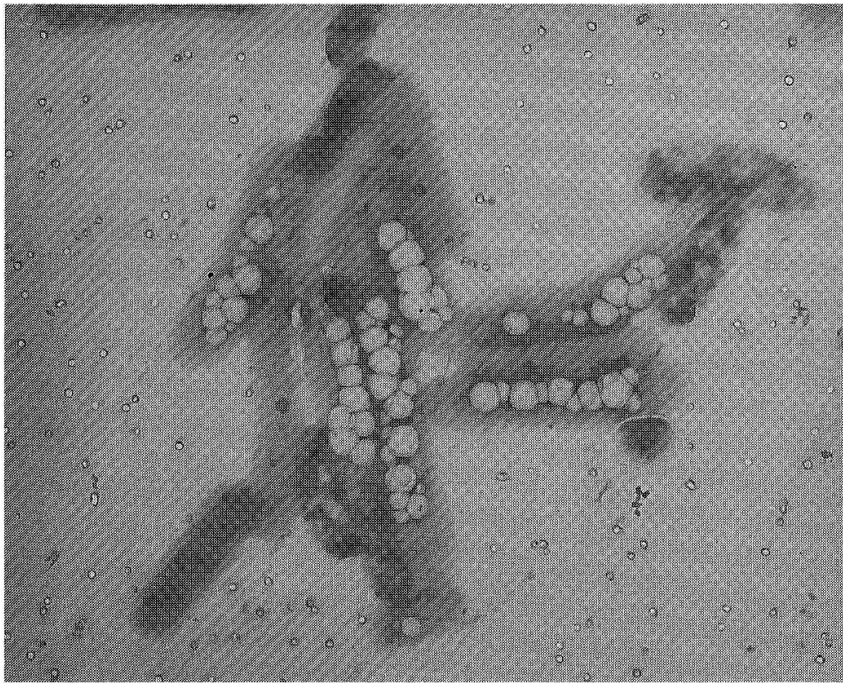
In the 1970's, a notion about a new form of water, called polywater, and its unusual properties caught tremendous interest among scientists, However, a more careful investigation of the phenomenon later established that the observations of "polywater" are due to silicon in laboratory glassware. To ensure that I_E Crystals are not related to a silicon contamination, the x-ray spectra of control pure water and I_E Crystal samples were examined (Figure 5). There were some particles of dirt observed in the purified water control sample. When the electron beam was focused on those particles, a characteristic Silicon peak was identified in the x-ray spectra obtained (Figure 5a). No such peak was detected when the electron beam was focused on any I_E cluster (Figure 5b), Therefore, I_E Crystals are far different from polywater,

3.3 Observation of three-dimensional Structure of I_E Crystals with AFM

The 3-D conformation and packing of I_E Crystals were studied on mica surface with NanoScope@ Multimode AFM (Digital Instruments, Santa Barbara, CA) in TappingMode™. AFM is a high resolution technique for studying surface topography and is used in a wide array of application areas, including biology, semiconductors, polymers, etc.

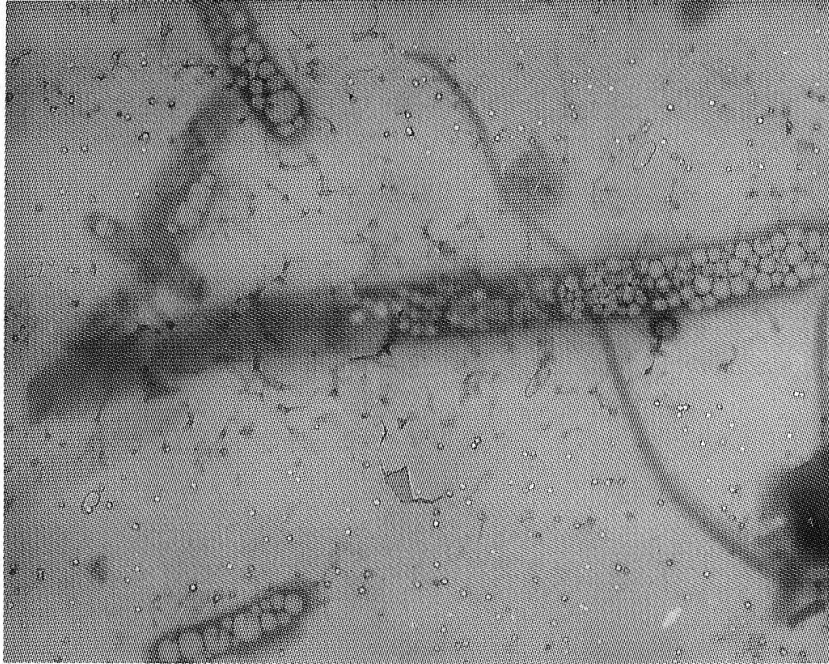


a.

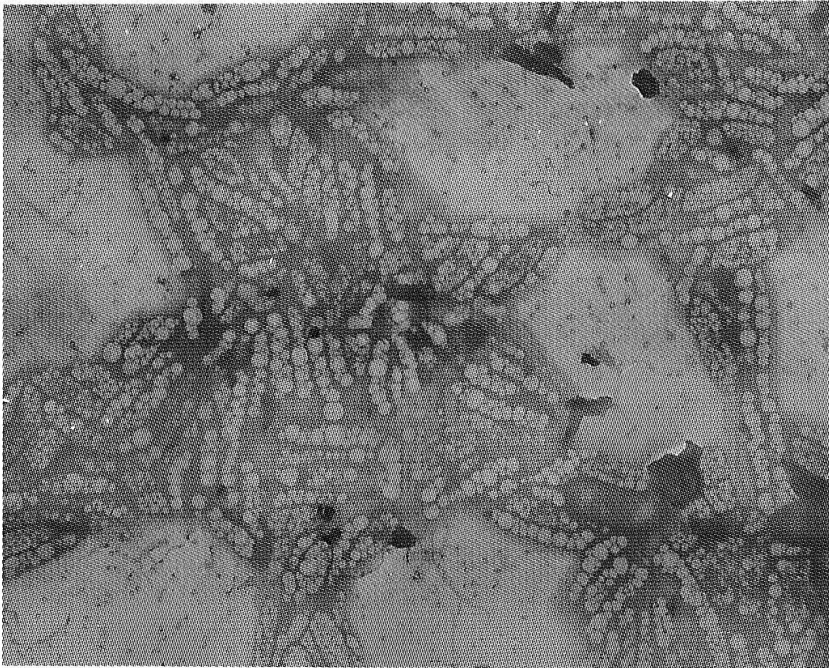


b.

Figure 4 (a,b) Electron Microscopy images of different I_E clusters obtained from different I_E solutions and prepared using different initiators: (a) Isomaltose, amplification 5.000x, (b) cellulose, amplification 5,000x.

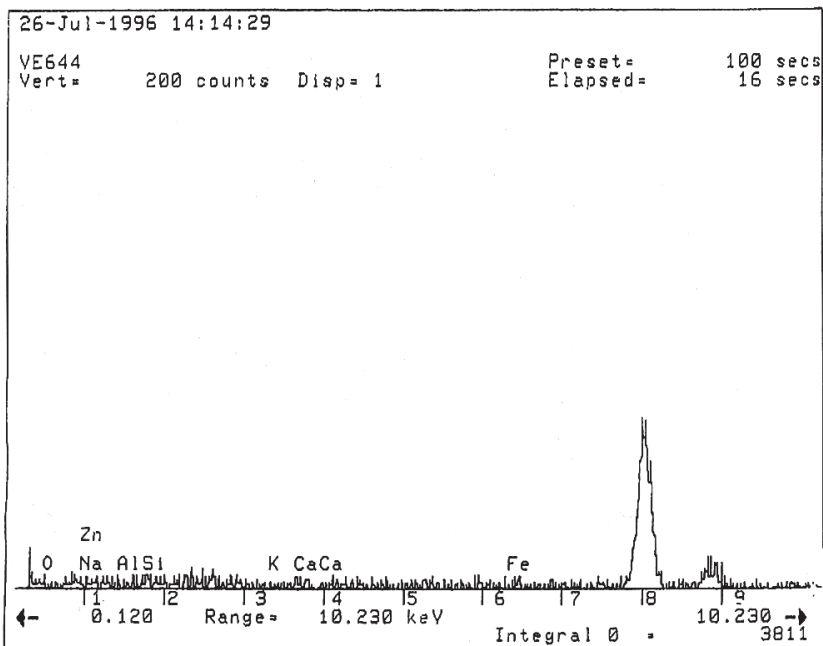


c.

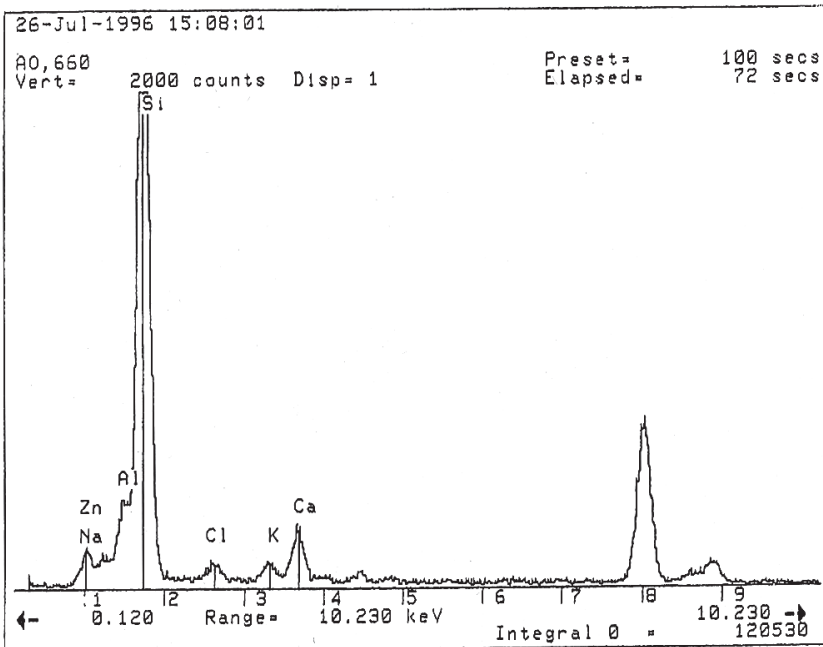


d.

Figure 2 Figure 4 (c,d) Electron Microscopy images of different I_E clusters obtained from different I_E solutions and prepared using different initiators: (c) sophorose, 6,000x, (d) DS, proprietary solution 3,500x. The Electron Microscope is Hitachi H600A, 100keV electron beam. The small holes in the images are filter paper hole of $0.1 \mu\text{m}$ size. Qualitatively the clusters look different.



a.



b.

Figure 5 X-ray spectra of control pure water and I_E sample. (a) A silicon peak was observed at approximately 1.7 keV when the electron beam was focused on a dirt particle in control water (b) No silicon peak was detected when the electron beam was focused on the I_E clusters. The peak at 8 keV is from the copper grid that holds the sample.

In this method, an oscillating cantilever with a sharp tip at the end is moved across the sample. A reduction in amplitude of oscillation, as the cantilever contacts the sample surface, is monitored with a laser beam focused on the back of the cantilever. The recorded information about changes in oscillation amplitude is then used to identify and measure surface features⁴⁰.

I_E Crystal samples were observed in two different ways. (1) A few drops of IE Crystal solution were placed on freshly cleaved atomic smooth mica substrate surface and were dried by heating the substrate with warm air. The height images of I_E adsorbates were then recorded (Figures 6a-c). (2) To avoid possible effect of drying on the structure of I_E clusters, a fluid cell was used. A fluid cell allows operation of an AFM with the sample and the scanning tip under a fluid. The I_E structures deposited on the bottom of the cell were then imaged in their natural fluid environment (Figure 6d).

Size distribution analysis of imaged I_E samples indicated three major sizes of I_E clusters: 10nm, 100nm and 1mm. The observed I_E clusters were shown to be relatively flat objects, with the heights of approximately 10% of their length.

4 Direct Evidence of the Electric Nature of the I_E Clusters

Three methods were used to establish the electric nature of I_E clusters:

- a. An observation of electric field lines emitted by I_E clusters.
- b. Analysis of nuclear magnetic resonance (NMR) spectra of I_E solutions.
- c. Measurements of resistivity and electromotive force (emf) of I_E solutions.

4.1 Evidence of Electric Field Emitted by I_E Clusters

The magnetic field of a magnet can be visualized by spraying iron powder around a magnet. Particles of the powder will align themselves along the magnetic field line emitted from the magnet. Similarly, electric field lines emitted by I_E clusters were observed as described below.

Monosodium phosphate, NaH_2PO_4 , was dissolved in water containing I_E Crystals, referred to as I_E water. A small amount of the solution was placed on a glass microscope slide and allowed to evaporate and crystallize. The slide was then examined with an optical microscope with a magnification of 100x. A control sample was prepared by dissolving the salts in deionized water (18 MW-cm, less than 10 ppb total dissolved solids). The monosodium phosphate crystals, precipitated from control solution, demonstrated no ordered pattern (Figure 7a). The monosodium phosphate crystals precipitated from I_E -based solution lined up in a straight line (Figure 7b).

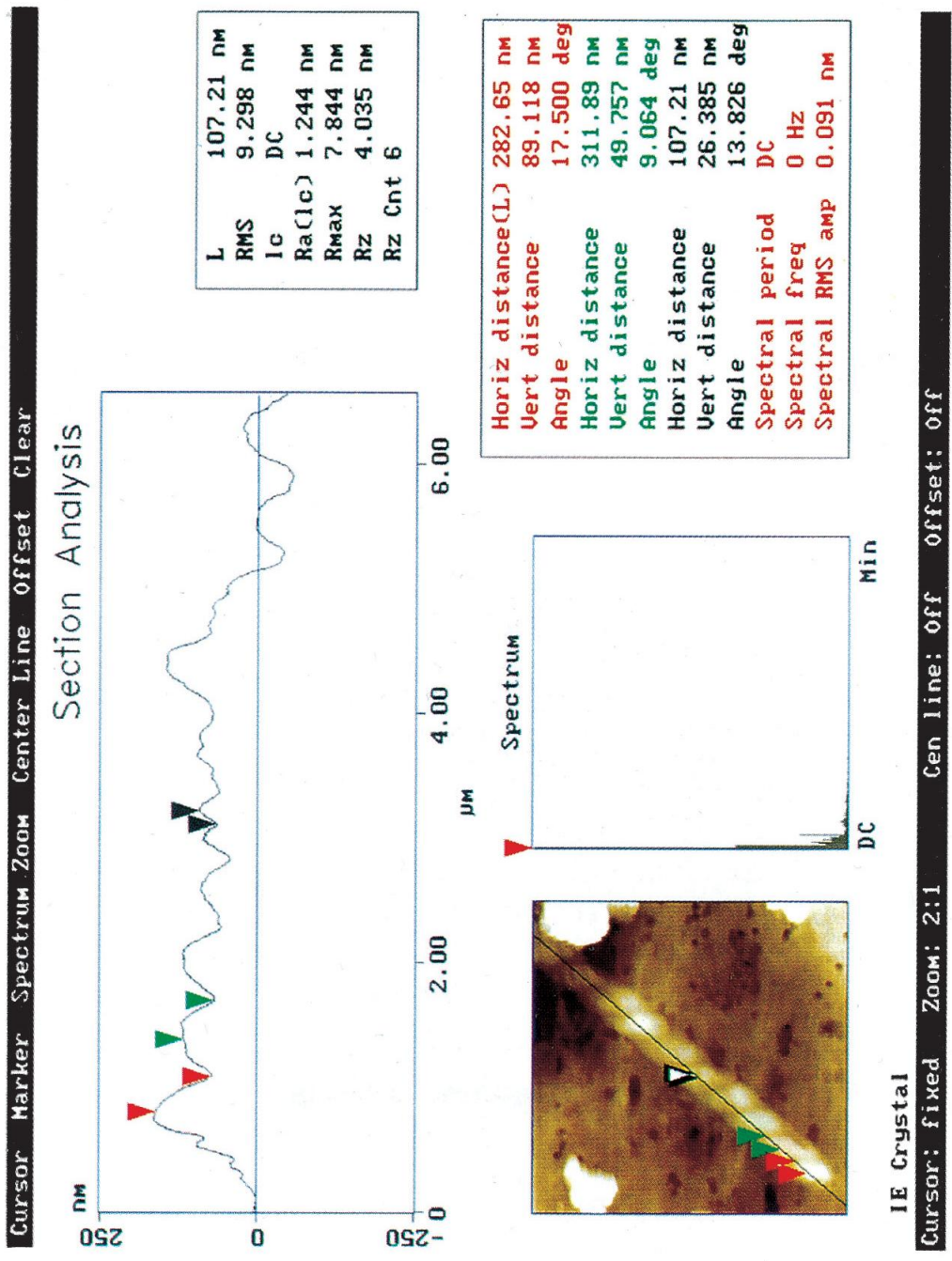


Figure 6a A 3-dimensional image of a micron size I_E clusters deposited on mica surface. The image was recorded in Tapping ModeTM with NanoScope AFM (Digital Instruments, Santa Barbara, CA).

NanoScope
Scan size 500.0 nm
Setpoint 0.5507 V
Scan rate 1.606 Hz
Number of samples 512

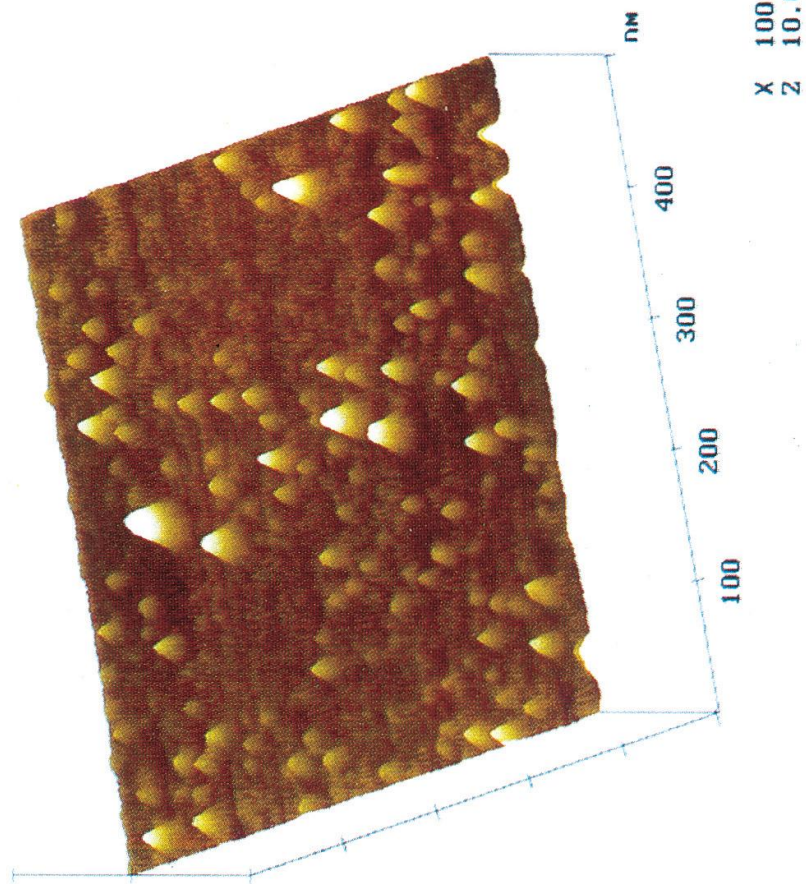
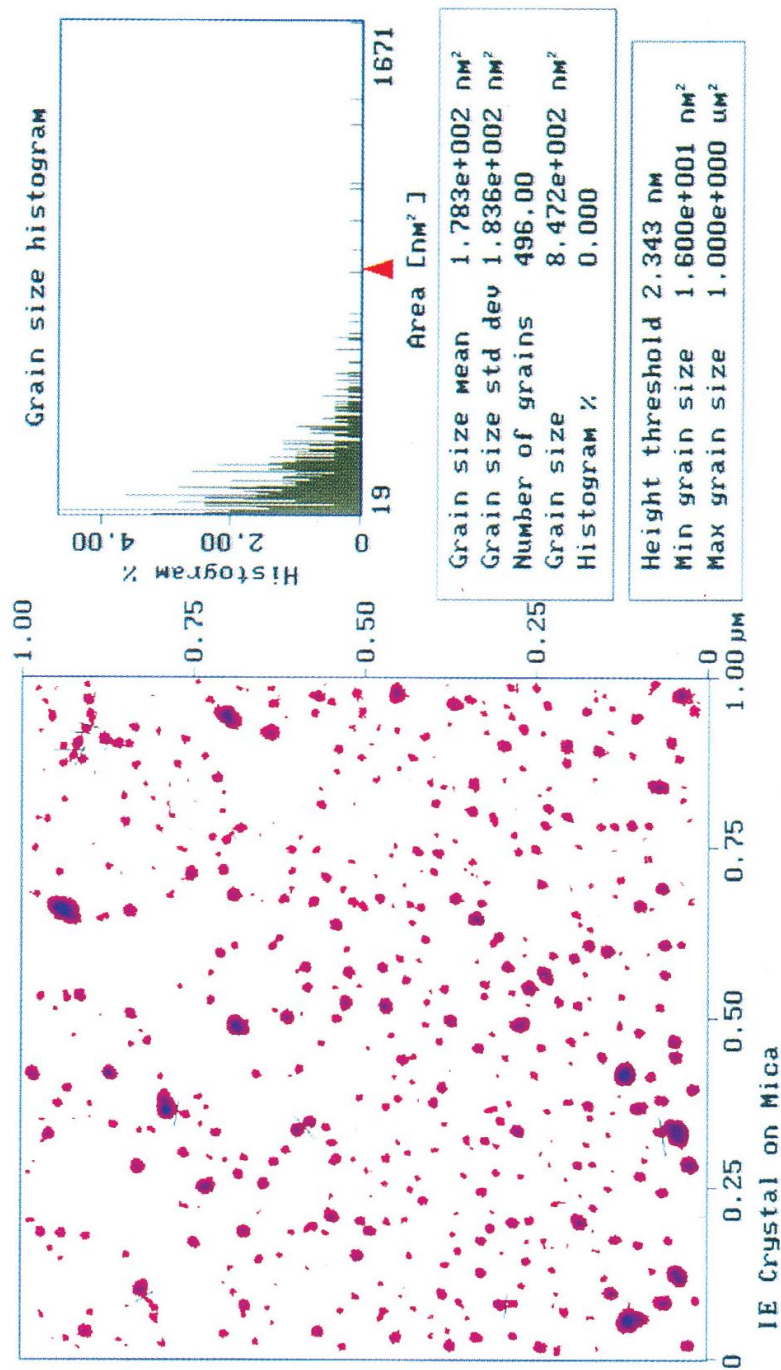


Figure 6b A 3-dimensional plot of ten nanometer size IE clusters deposited on mica surface. The image was obtained in Tapping ModeTM with NanoScope AFM (Digital Instruments, Santa Barbara, CA).

Image Threshold hist. Grain size hist Execute Limits Clear

Grain Size Analysis



Normal Image Bnd. Grains off

Figure 6c A 2-dimensional plot and a size distribution graph of small, ten nanometer size I_E clusters Deposited on mica surface The data was obtained by Tapping ModeTM scanning of I_E precipitate surface with NanoScope AFM (Digital Instruments, Santa Barbara, CA).

NanoScope
 Scan size 3.000 μm
 Setpoint 0.5281 U
 Scan rate 2.001 Hz
 Number of samples 256
 Tapping AFM

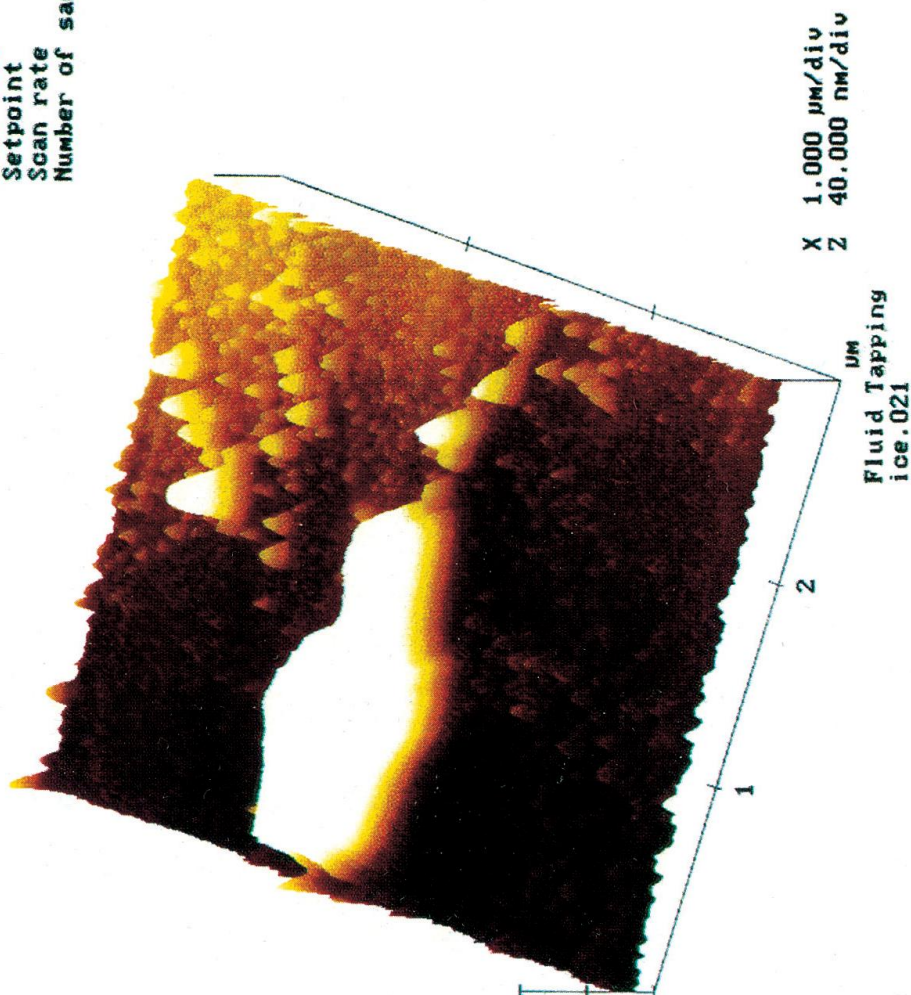


Figure 62 Three sizes of I_E clusters: hundreds of nanometer, and tens of nanometer size are all displayed together in this image recorded in a fluid cell with NanoScope AFM (Digital Instruments, Santa Barbara, CA).

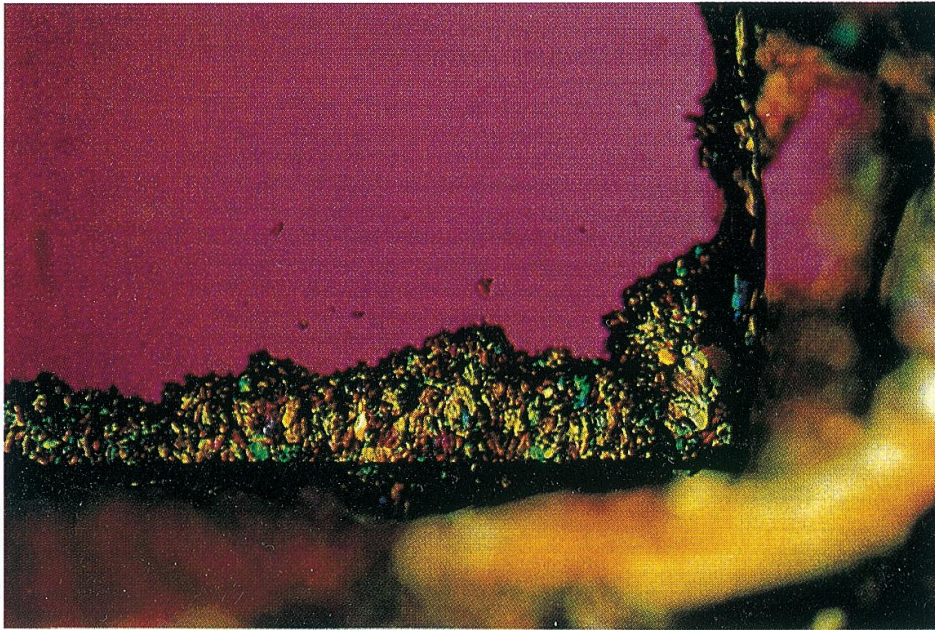
These results strongly suggest that molecules, in this case molecules of monosodium phosphate, prefer to line up along the minimum energy position, which corresponds to the electric field lines emitted from the I_E clusters.

In order to further confirm the electric nature of IE clusters, an external electric field of 20 volt/in or 100 volt/in was applied during the crystallization process. The electric field did not have any effect on the formation of monosodium phosphate crystals in control water solution (Figure 7c). However, the monosodium phosphate crystals, precipitated from I_E -based solution, aligned along the direction of the external electric field (Figures 7d and 7e). These observations can be explained by an interaction between the external electric field and the electric dipole moment of I_E clusters. The I_E clusters rotate, to align themselves with the external electric field, in order to stay at the minimum energy configuration and serve as nuclei for monosodium phosphate crystallization. Control water, on the other hand, does not contain I_E clusters, so there are no permanent net electric dipole moments available for an interaction with an external electric field. Therefore, no alignment of the monosodium phosphate crystals is observed in the case of control water.

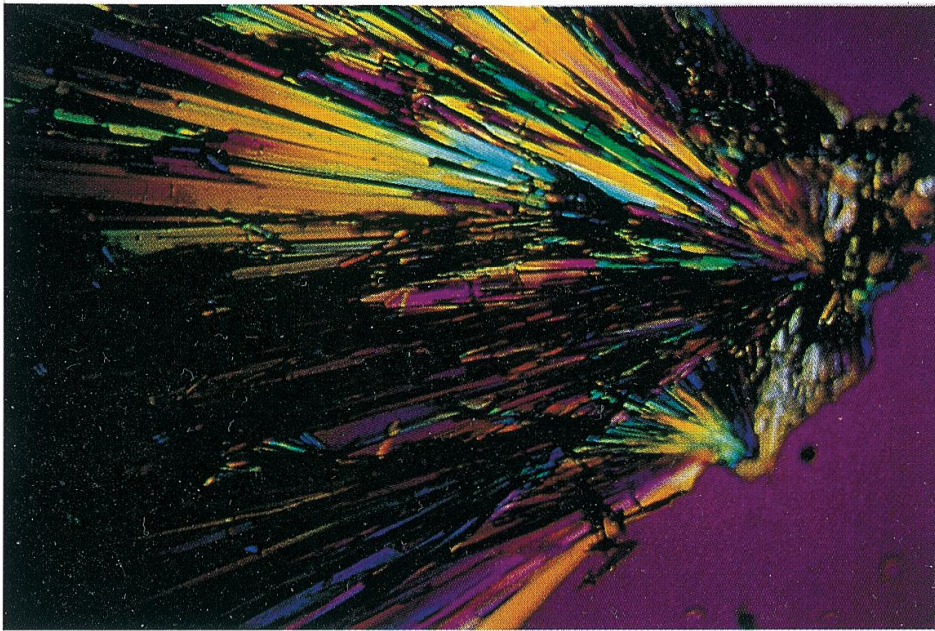
X-ray diffraction analysis was carried out on powdered monosodium phosphate crystals precipitated from control and I_E waters. The original monosodium phosphate reagent (Sigma, St. Louis, MO) was also analyzed. The positions of the observed x-ray diffraction peaks (Table 2) were compared to the JCPDS-ICDD standard, that provides fingerprint information on various crystals. The original sample was, as expected, anhydrous. The crystals obtained from control water solution were monohydrates (NaH₂PO₄·H₂O), and the crystals precipitated from IE -based solution were dihydrates (NaH₂PO₄·2H₂O), This data indicates a difference in the crystallization process in the presence and in the absence of I_E Crystals.

4.2 A Shift of Proton Peak Position in NMR Spectra of I_E Solutions

To demonstrate that water molecules inside I_E clusters arrange themselves differently from water molecules in ordinary water, the positions of protons in water molecules were measured by NMR. NMR is a very sensitive way to detect the change of environment that protons find themselves in, since the method allows separation of signals from water and contaminants.

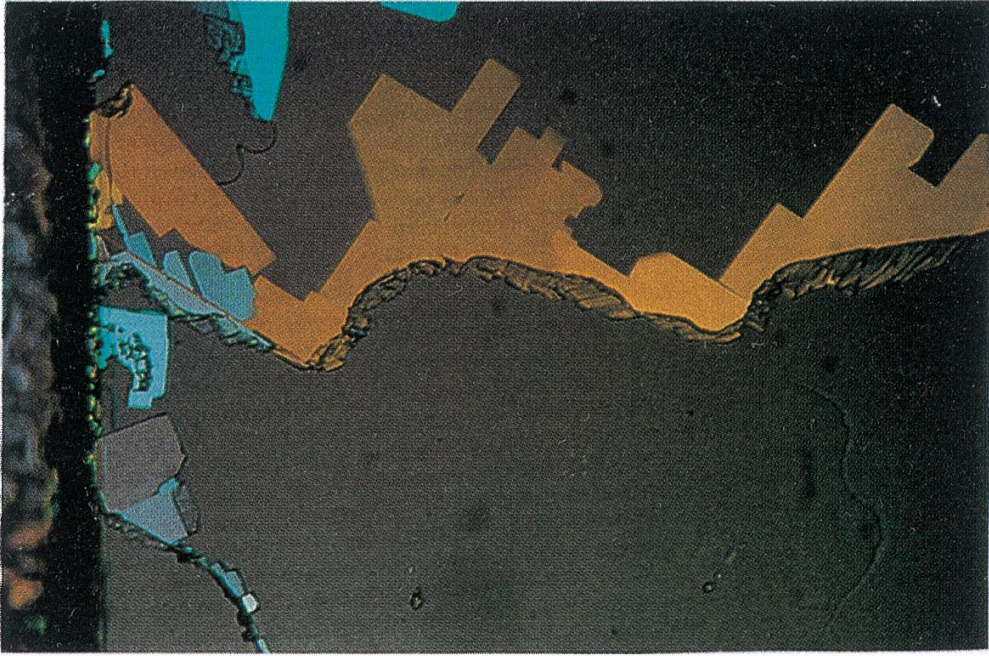


a

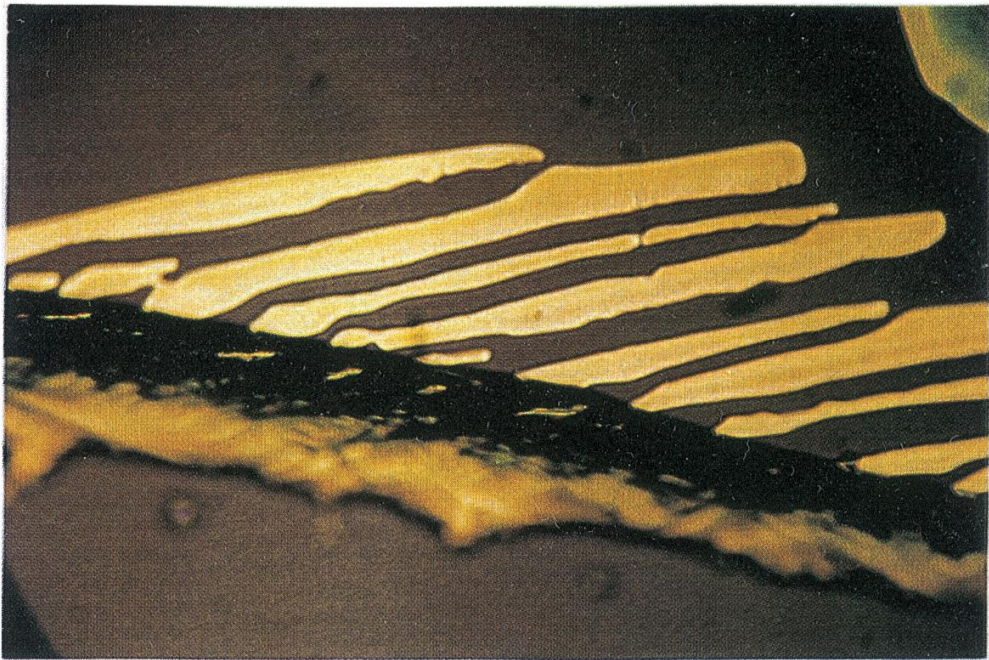


b.

Figure 7(a, b) (a) Monosodium phosphate crystals precipitated from control water solution. No obvious pattern was observed. (b) Monosodium phosphate crystals precipitated from I_E -based solution. The observed radial lines were interpreted as due to electric field lines from the dipole of I_E clusters.



c.



d.

Figure 7(c, d) (c) No regular pattern was observed for the growth of monosodium phosphate crystals Item control solution. (d) Sodium monophosphate crystals grew along the external electric field line, when a DC voltage of 100 volts was applied across the one inch slide containing I_E -based solution. The photograph was taken 3 hours after the beginning of the crystallization.

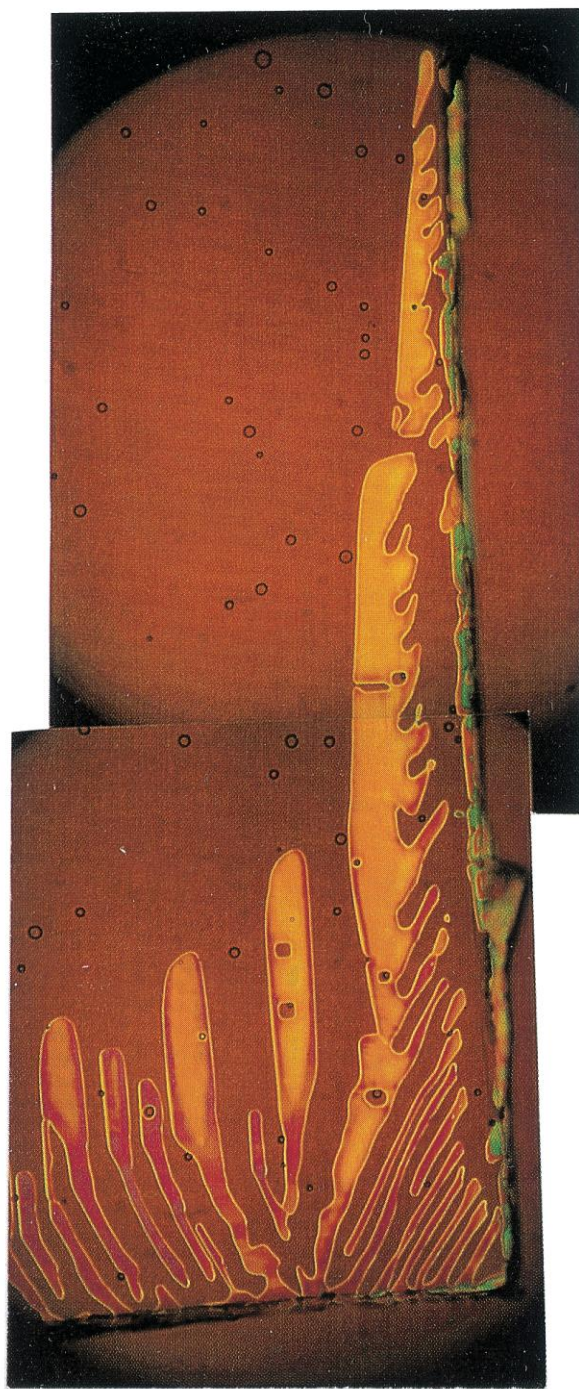


Figure 7(e) Sodium monophosphate crystallized from I_E -based solution in external electric field. The photograph was taken 20 hours after the beginning of the crystallization.

Table 2 X-ray diffraction peak(20₀)* of sodium phosphate crystals

Original sample	Crystals from deionized water solution	Crystals from IE water
NaH ₂ PO ₄ monoclinic	NaH ₂ PO ₄ .H ₂ O orthorhombic	NaH ₂ PO ₄ .H ₂ O orthorhombic
21.8	16.50	14.60
22.5	24.20	15.61
24.3	25.45	18.20
25.2	26.45	19.90
26.4	28.20	24.19
27.0	29.22	24.60
28.2	32.80	27.10
29.0	33.85	29.30
30.2	35.00	29.90
31.5	35.40	31.40
33.0	36.20	31.60
		33.80

* X-ray radiation CuKCl; lambda1.5405

The electro-magnetic wave with frequency ω will be absorbed by the proton with magnetic moment μ in a magnetic field B . as it obeys the following law (1):

$$\hbar\omega = \vec{\mu} \cdot \vec{B} \quad (1)$$

$$\omega = \omega_0 + \omega_1 + \omega_2 \quad (2)$$

$$\vec{B} = \vec{B}_0 + \vec{B}_1 + \vec{B}_2 \quad (3)$$

where ω_0 is the resonance frequency of a free proton in vacuum with an external magnetic field B_0 . The additional magnetic field B_1 comes from electric current, caused by the electron cloud surrounding the proton, in ordinary water. A 500 MHz resonance in vacuum, produces a shift in ω_1 of approximately 2400 Hz for a proton in water. When water molecules rearrange themselves to form a larger electric dipole moment, one expects that the electron cloud would be pulled away from its normal position in ordinary water. The change of electron cloud position will cause a change in magnetic field, which is defined as B_2 . The change in magnetic field will cause additional shift in frequency ω_2 that can be registered by NMR (Figure 8).

Principle of NMR

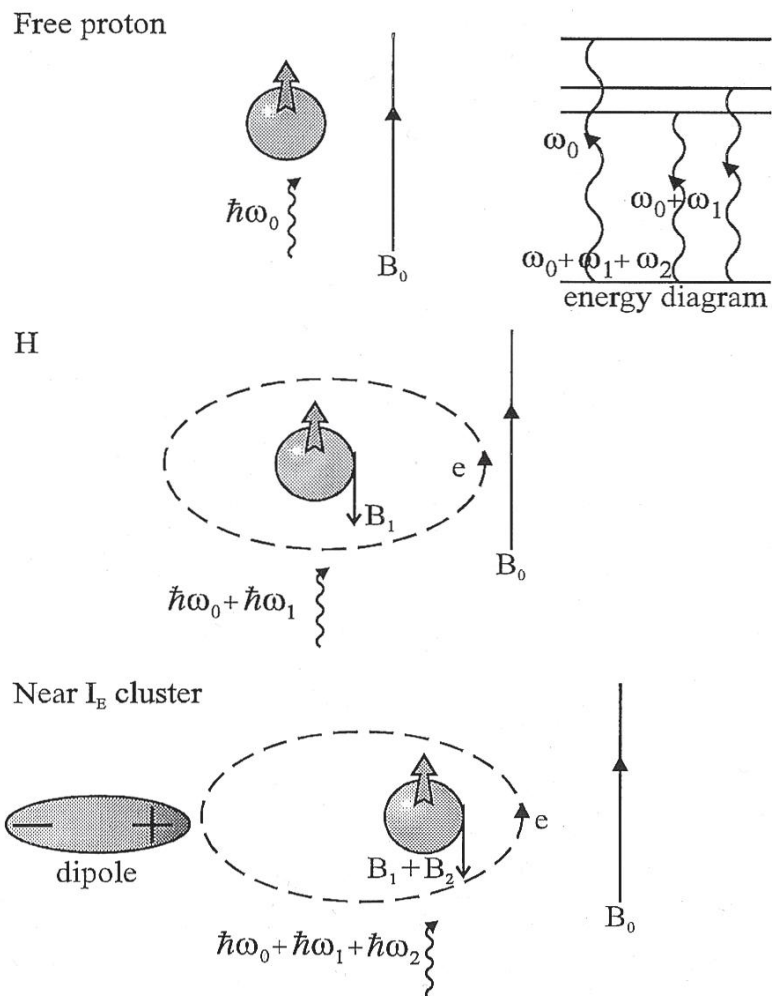


Figure 8 The principle of NMR method. A free proton under external magnetic field B_0 , has a resonance frequency of $\hbar\omega_0$.

It is not possible to precisely calculate the value of the shift ω_2 without extensive computer calculations and detailed knowledge of the electron wave function. However, one can attempt to understand the shift in the following way. Assuming a linear relation between the electric field, E , felt by an electron to the magnetic field, B , felt by a proton, the relationship (4) can be written:

$$B_1 / B_2 = E,$$

where E_1 is the an electric field on electron in hydrogen atom, and E_2 is the electric field that comes from the electric dipole moment of an adjacent water molecule. In normal water E_2 cancels out. However, in the I_E cluster, the parameter is not negligible.

$$\boxed{E_1 = e / r_0} \quad (5)$$

$$E_2 = \eta e r_0 / r^3 \quad (6)$$

where e is an electron charge, r_0 is the radius of hydrogen atom 0.51 \AA , r is the size of water molecule (0.28 nm), and $\eta e r_0$ is a permanent electric dipole moment of water clusters, η is a scale factor.

Therefore, $E_1 / E_2 = \eta (r_0/r)^3$ is on the order of several parts in thousand if $h \sim 1/10$. From this rough estimate, it is expected to get a shift of several Hz using a 500 MHz NMR.

A very concentrated I_E water solution contains more than 10% of I_E clusters. Water molecules in an I_E solution can be inside or outside of I_E clusters. A proton inside an I_E cluster will be affected more than a proton of bulk water molecules by the permanent electric dipole moment of I_E clusters. Therefore, two different shifts in proton peak position are expected.

It is proposed, that the smaller the I_E cluster, the larger the electric dipole moment. When two I_E clusters of the same size and same electric dipole moment come together, the lowest energy state for them is the one when a larger cluster is formed from two smaller ones, so that the two electric dipole moments align opposite each other with a net zero electric dipole moment. Therefore, the larger association of the I_E clusters, the smaller its electric dipole moment.

In order to maximize the influence of electric dipole moment on a proton, a concentrated I_E solution (P1) was sonicated by ultrasound for 1.5 minutes, and the NMR spectrum was recorded at timed intervals. A shift in proton peak position of water was observed immediately after sonication and became smaller over time (Figure 9a). These results can be related to the breakage of large I_E Crystals by sonication, with their further spontaneous recombination (Figure 10), similar to the phenomenon observed in the laser autocorrelation experiments. No shift was detected in control water (Figure 9b). Less concentrated I_E solutions, P2 and P3, were studied with NMR. P2 and P3 were, respectively, 10 and 50 times less concentrated than P1 solution. A dependence of the magnitude of proton peak shift on I_E Crystals concentration was established (Figures 9a, c, d).

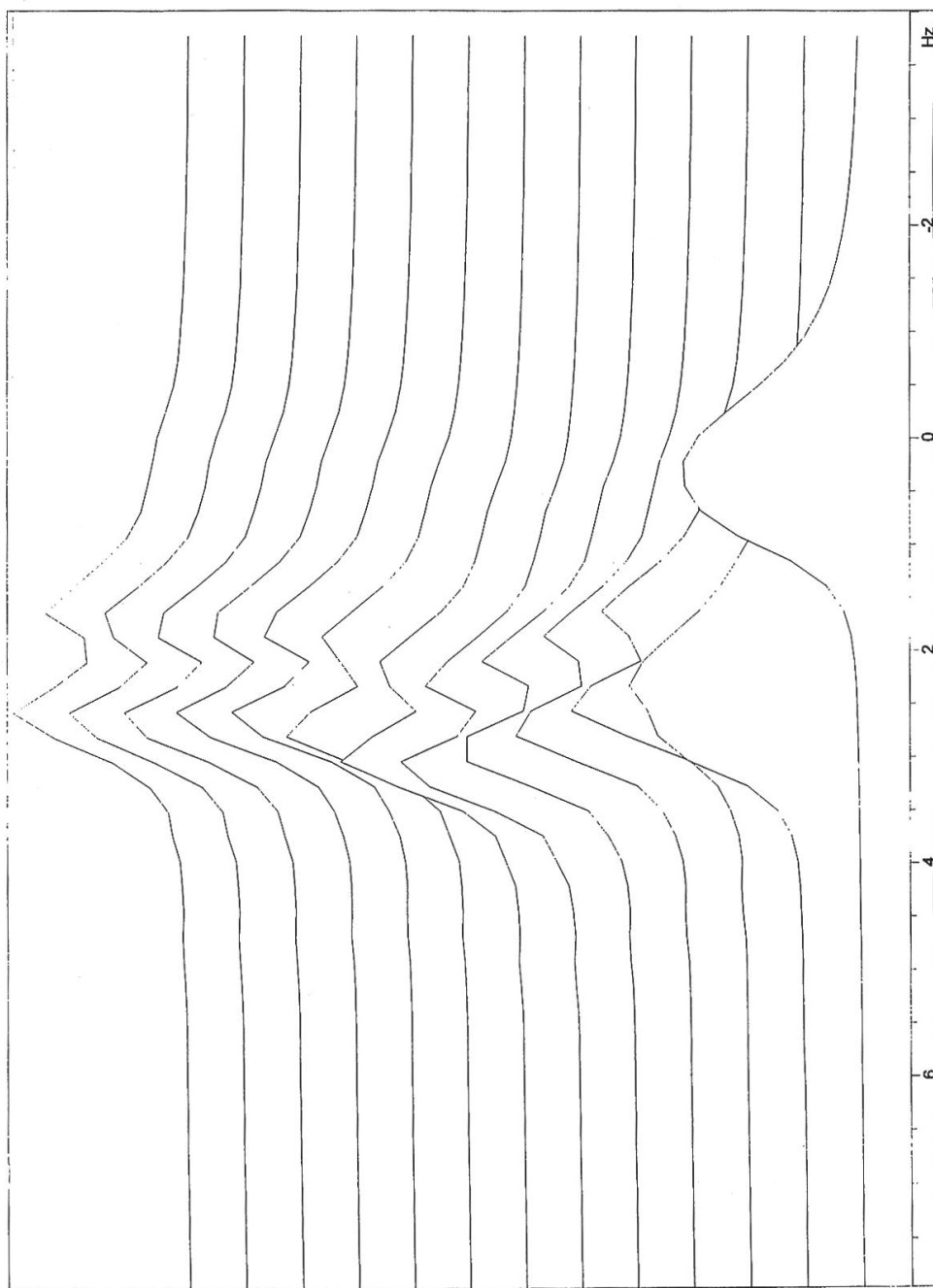


Figure 9a A concentrated I_E solution (P1) was studied by NMR prior to the sonication which shown in the bottom curve. After a 1.5-minute sonication, the next 12 spectra (from the bottom to the top) were measured in time intervals of 2 min., 4 min. x 6.9 min., 6min., 8 min., and 7 min. respectively. A proton peak shift of approximately 3 Hz was observed.

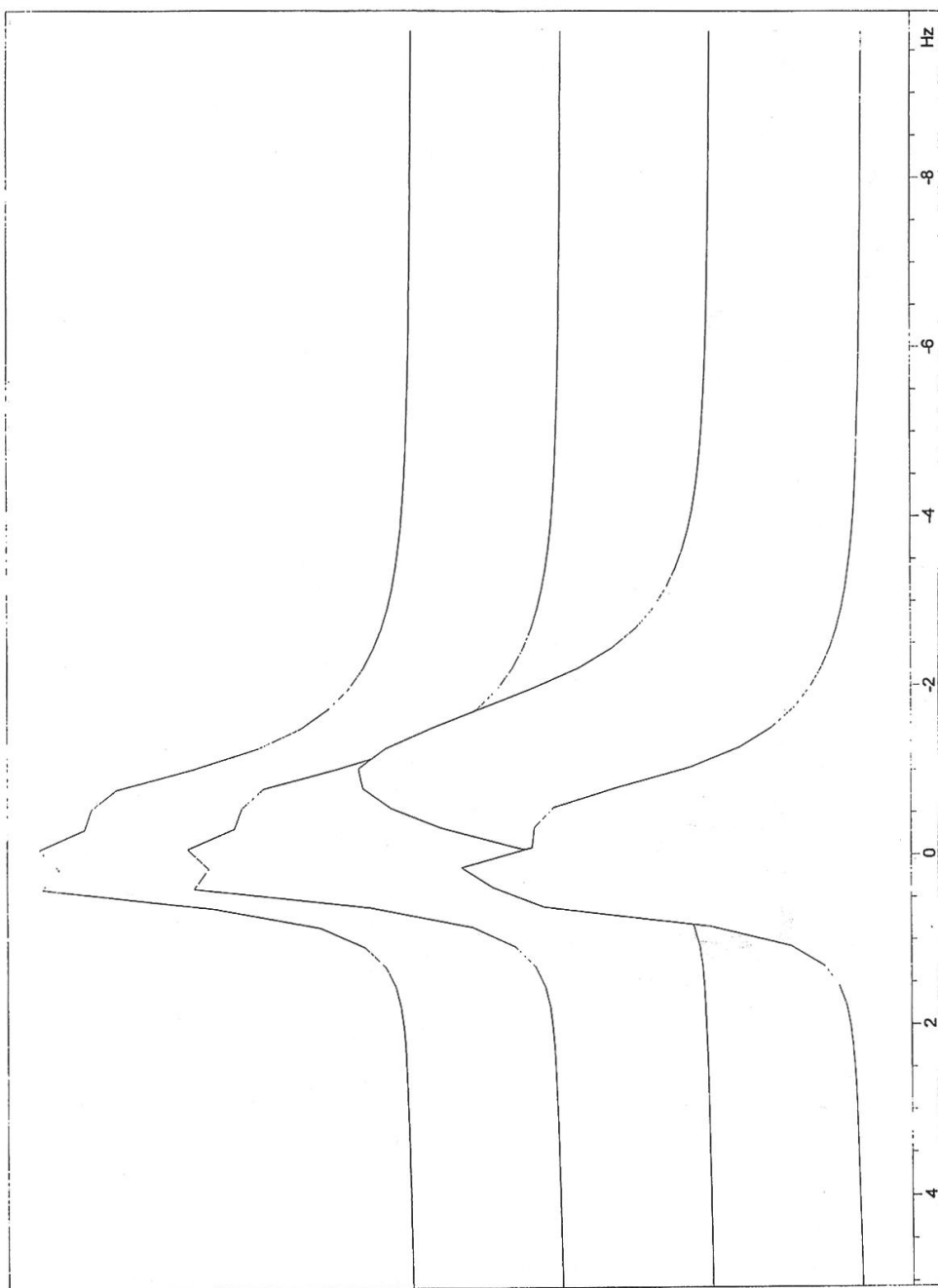


Figure 9b A sample of control water was studied by NMR. The bottom spectrum was recorded prior to the sonication. After a 1.5-minute sonication, the next three spectra were measured in time intervals of 2 min., 5 min, and another 5 min. respectively. the top two curves are the same as before shaking, as expected, with no observed proton peak shift.

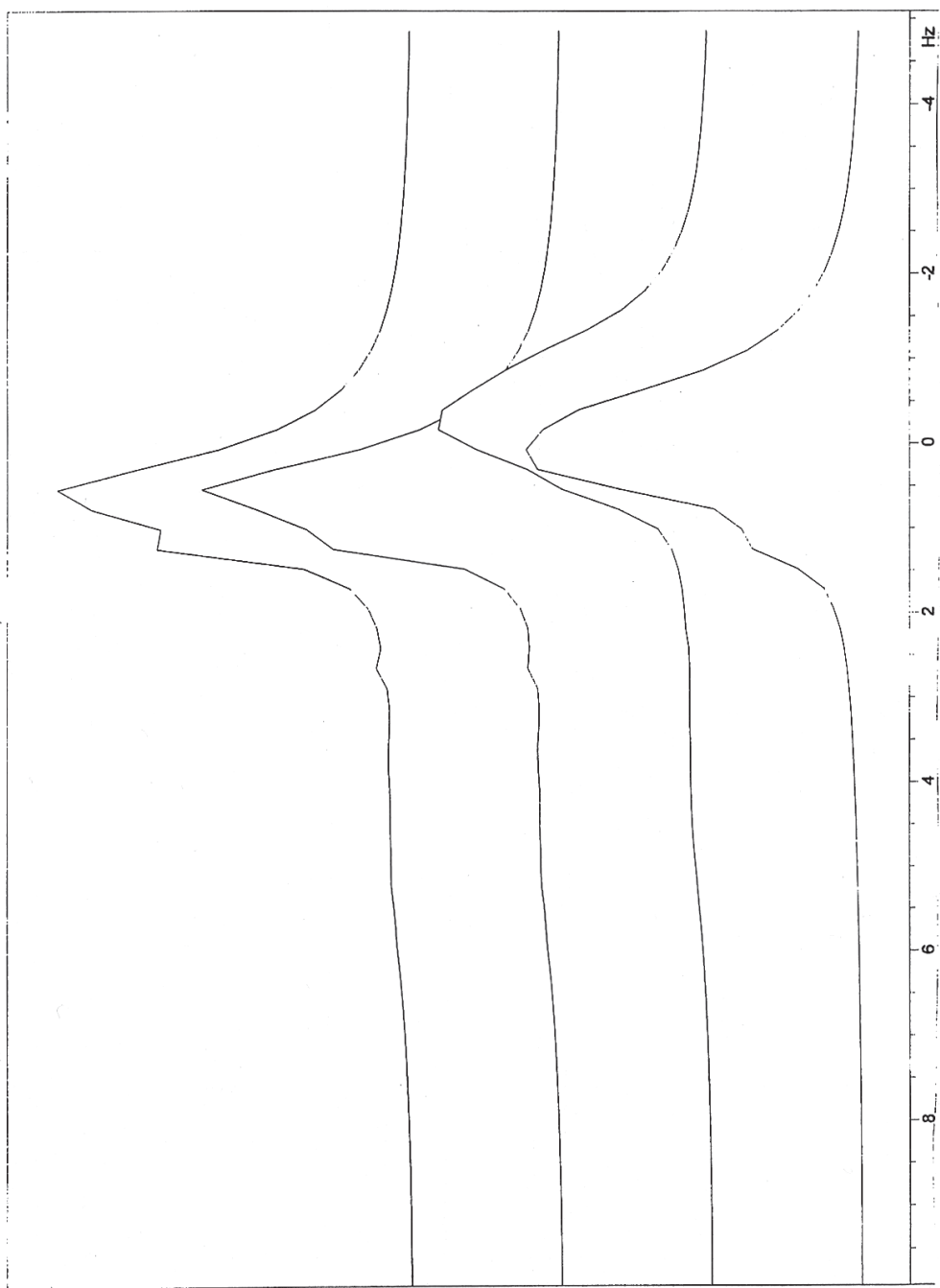


Figure 9c A sample of low concentrated I_E solution (P3) was studied by NMR. The bottom spectrum was recorded prior to the sonication. After a 1.5-minute sonication, the next three spectra were measured in time intervals of 2 min, 3 min., and 4 min respectively. The top two curves demonstrate a proton peak shift of 0.5 Hz.

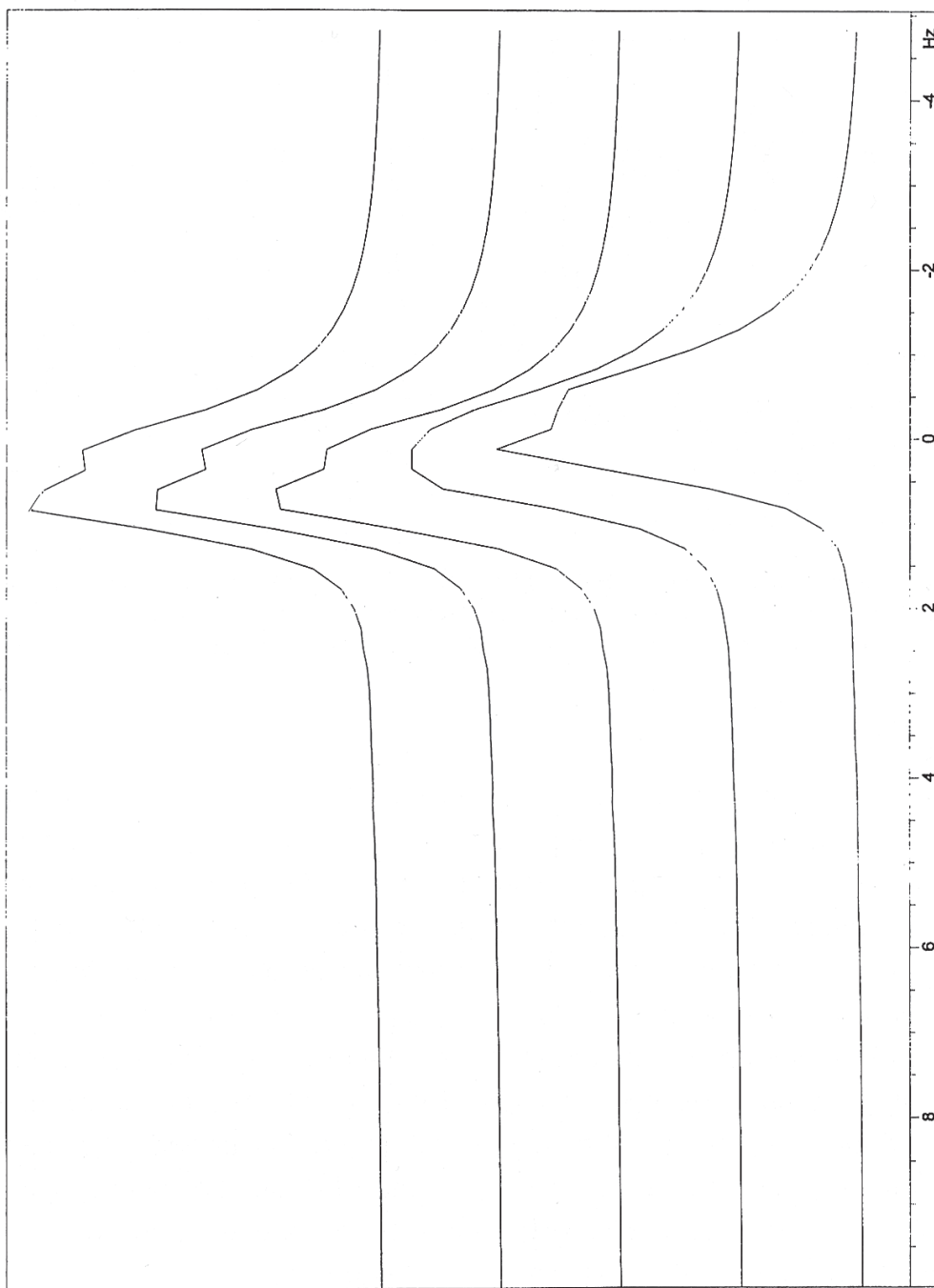


Figure 9d A sample of medium concentrated I_E solution (P2) was studied by NMR. The bottom spectrum was recorded prior to the sonication. After a 1 5-minute sonication, the next four spectra were measured in time intervals of 1 mix, 4 min., 4 min., and 3 min, respectively. A proton peak shift of 1.5 Hz was detected.

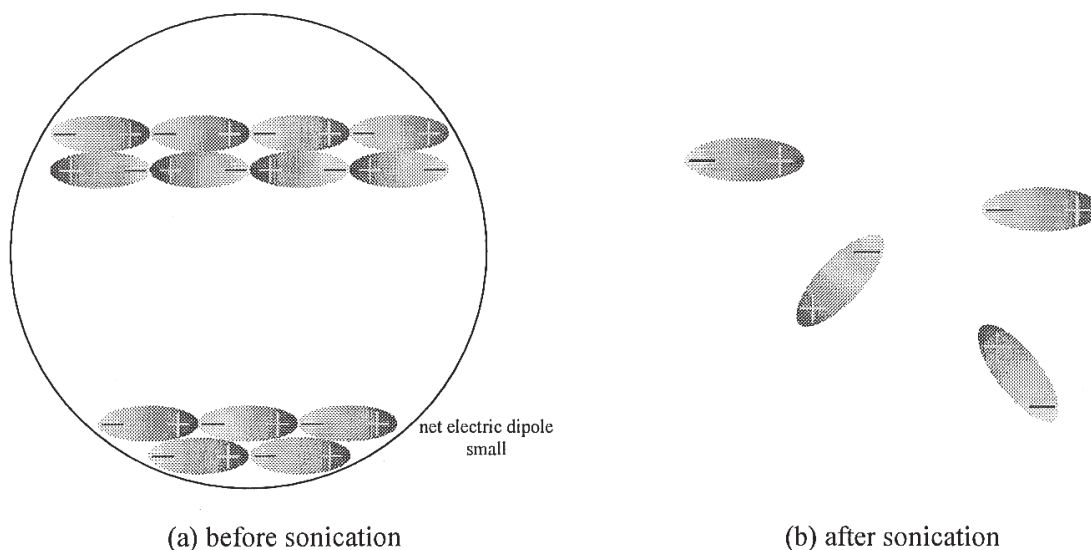


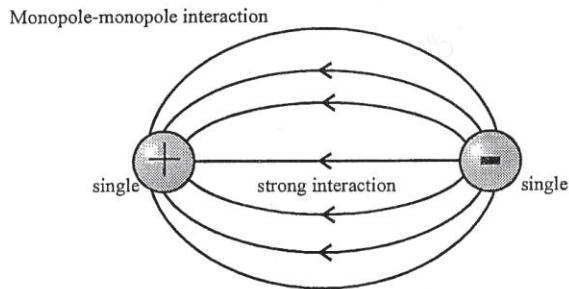
Figure 10 A large I_E cluster composed of smaller clusters has a small net electric dipole moment before sonication due to cancellation of the individual electric dipole moments (a), Sanitation breaks the large I_E cluster into many smaller ones (b), and as a result a larger net electric dipole moment is produced.

4.3 Electric Potential Measurement

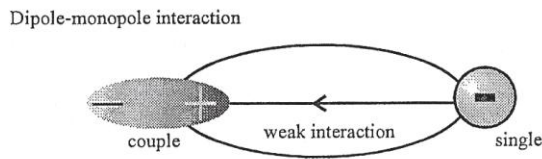
A strong electrostatic attraction is known to exist between ions, or monopoles, of the opposite charge, e.g. a positive ion Na^+ is strongly attracted to a negative Cl^- ion. Water molecules are dipoles, with one part of the molecule carrying a partial positive charge and the other a partial negative charge. An attraction force between a dipole and a molecule exists, but it is much weaker as compared to an attractive force between two monopoles. The attraction between water molecules in an I_E cluster is of dipole-dipole type and it is the weakest. An anthropomorphic analogy can be made. A single male and a single female are like monopoles of the opposite charge and they are strongly attracted to each other. A married man is a part of a couple (dipole), however, he can be also attracted to another woman (monopole), but such attraction is less. The attraction between two married couples (dipole-dipole interaction) is, of course, the weakest (Figure 11).

Previous studies³⁷ have reported that an emf of tens of mV was observed between two stainless steel electrodes immersed in I_E solution. In ordinary ionic solutions, no emf is established between two identical electrodes. However, in the case of I_E solutions, the electric dipoles of the I_E clusters can line up to establish an emf without any electrochemical reaction occurring.

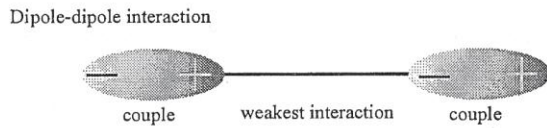
In this study we used a pH meter (Fisher Scientific, PA) to measure an electric potential established by the electric dipole of the I_E clusters (Figure 12).



(a) A single man (monopole) is strongly attracted to a single girl (a monopole with an opposite charge).

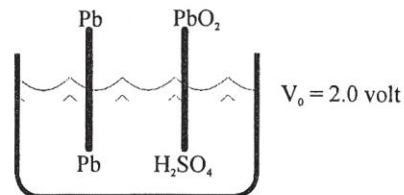


(b) The attraction between a married man, part of a couple (electric dipole) to a beautiful girl (monopole) is weaker.



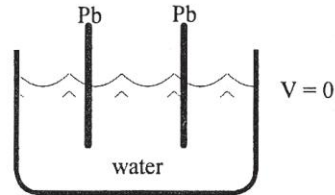
(c) The attraction between two married couples (two water clusters dipoles) is the weakest.

Figure 11 Attraction between monopoles and dipoles.

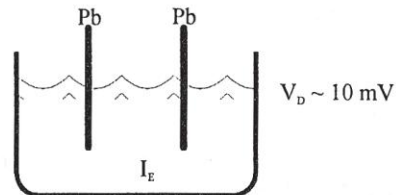


lead battery in sulfuric acid

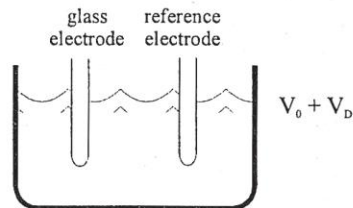
(a) A lead battery has a potential of 2.0 volt.



(b) Two lead electrodes in water have zero potential.



(c) Two lead electrodes in I_e water should have potential of $\sim 10\text{mV}$.



(d) Two electrodes, a glass electrode and a reference electrode of a pH meter, were used to measure dipole electric potential of an I_e solution.

Figure 12 Measurement of dipole electric potential

The electric potential between a glass electrode and a reference electrode is given by the Nernst equation (7).

$$E = E^0 + (2.3R T_k / nF) \text{Log } a_i \quad (7)$$

where E^0 is the standard redox potential; R , gas constant, has a value of $8.314 \text{ Jmol}^{-1}\text{K}^{-1}$; F , Faraday constant, has a value of $96,490 \text{ Cmol}^{-1}$; T is absolute temperature; n is a number of electrons transferred in the reaction; a_i represents activities of participating species. We expect that the electric potential of an I_E solution will differ from the electric potential of ordinary water due to the additional contribution of the aligned electric dipole moments of Ia_i clusters:

$$E(I_E) = E + ED \quad (8)$$

where ED is additional electric potential produced by dipole moments of I_E clusters.

We used a pH meter to study a deviation from the linear relationship between electrode potential and pH (9) in I_E solutions.

$$\text{pH}(X) = \text{pH}(S) + 1/k[E(X) - E(S)] \quad (9)$$

where S denotes a pH standard used to calibrate the pH meter; X is a sample; $k = R \ln 10 / F = 59.2 \text{ mV}$ at 25°C .

A wide range of pH, from $\text{Ph}=1$ to $\text{Ph}=12$ was analyzed. The test solutions were prepared either with concentrated aqueous I_E solution (UV absorbance of 2 at 195 nm, $A_{195}=2$) or deionized (DI) water. The desired pH was obtained with hydrochloric acid or sodium hydroxide. The maximum deviation from the linear dependence between pH and E was observed at neutral pH, where dipoles strongly dominate the system's electric potential. The relative effect of electric dipole diminished at the extreme ends of the pH scale, where ionic (monopole) contribution dominates the potential (Figure 13). The addition of KCl (final concentration of 0.01 M) to I_E water-based solutions did not significantly change the shape of the pH-mV curve. Therefore, the electric potential of dipoles was not effected by the presence of additional ionic species. A linear relationship was found between electric potential and pH measurements in the case of control water for all pH values tested.

To study the effect of the solution's ionic strength on the observed phenomenon, a wide range (from 10 mM to 0.1 mM) of NaCl and KCl concentrations in I_E and water solutions were tested. The average difference in measured electric potential between water- and I_E -based solutions was 92.4 mV for NaCl and 103.4 mV for KCl (Table 3).

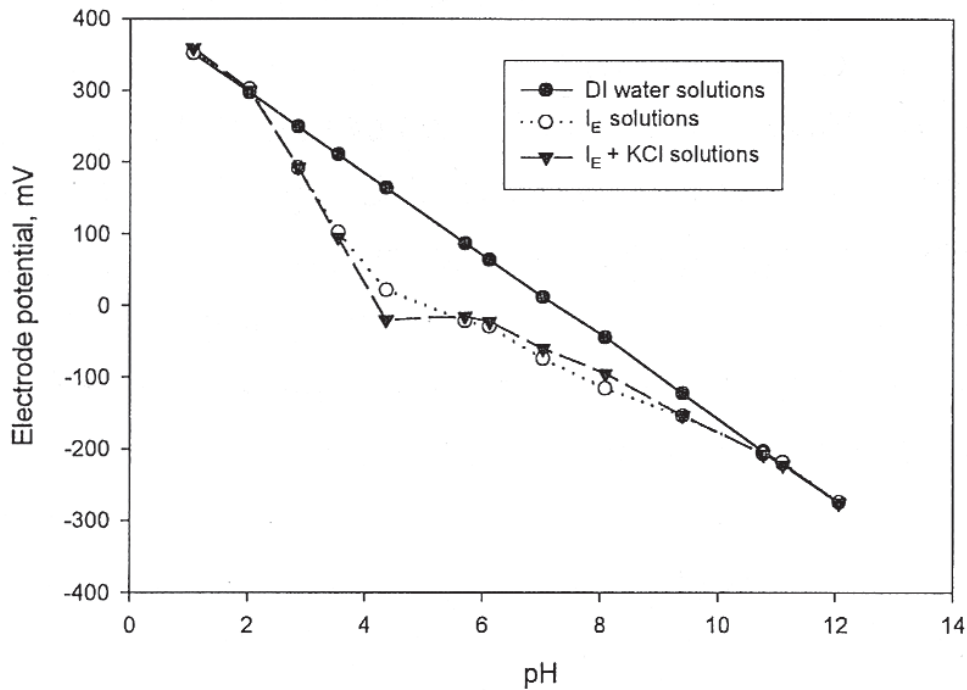


Figure 13 Electric potential of DI water and IE Water solutions.

	DI+NaCl		I_E +NaCl		DI+KCl		I_E +KCl	
	pH	mV	pH	mV	pH	mV	pH	mV
0.00001M	5.67	89.2	7.30	-4.1	5.60	92.7	7.30	-5.2
0.0001M	5.69	87.6	7.30	-3.8	5.65	98.4	7.42	-11.1
0.001M	5.65	90.0	7.29	-3.9	5.65	90.0	7.50	-15.6
0.01M	5.67	89.4	7.24	-0.8	5.61	91.7	7.54	-17.8
Average	5.67	89.2	7.28	-3.15	5.63	91.0	7.44	-12.4

Very little variation in pH readings for different concentrations of NaCl and KCl was observed, However, it is important to note that the large difference between the pit of DI water and I_E solutions (Δ pH - 7.28 - 5.67 1.61 (NaCl) and Δ pH - 7.44 - 5.63 - 1.81 (KCl)) measured by pH-meter, was not detected by pH 0-t4 indicator paper (VWR, West Chester, PA) and showed identical pH values for DI and I_E solutions. This observation can be explained by differences in the methods used for pH determination. A pH-meter is based on an electrochemical process. Since I_E Crystals produce an additional electric potential, the pH readings are affected. A chemical reaction takes place with pH paper, which is not influenced by the electric dipoles of I_E clusters.

The differences in electric potentials of water and IE solutions were analyzed for concentrated ($A_{195}=2$) and diluted ($A_{195}=0.8$) I_E solutions. A greater difference in electric potential, covering wider range of pH, was found in the case of more concentrated IE solution (Figure 14).

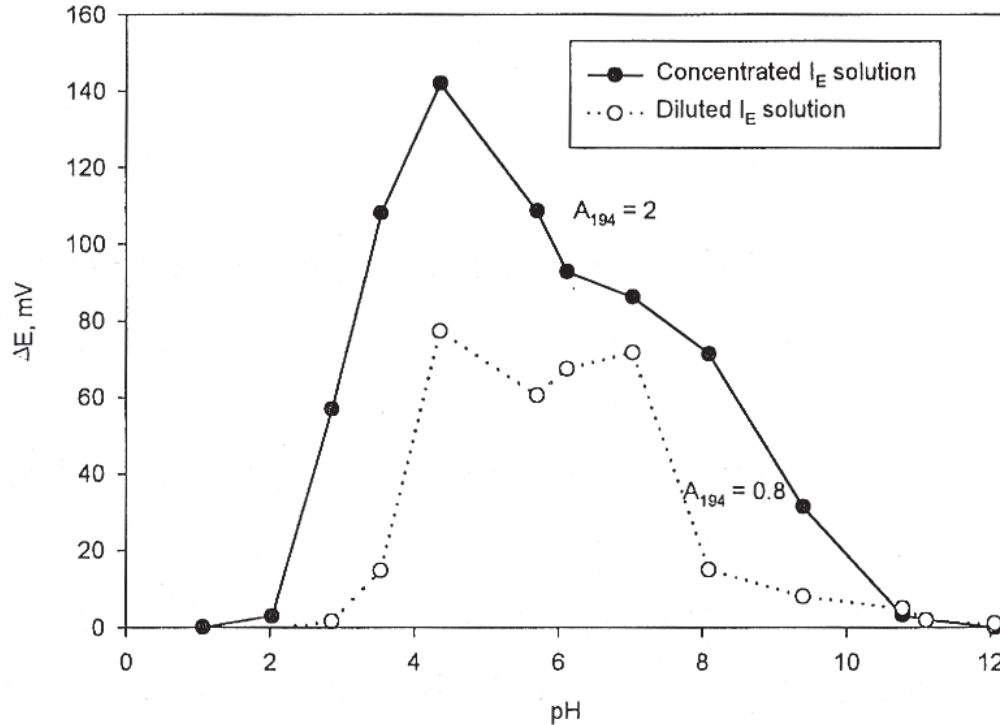


Figure 14 The difference in electric potential between I_E water and DI water versus pH. The more concentrated IE solution has a larger dipole potential than the diluted I_E solution.

The UV absorbance at $\lambda=194$ for deionized water and I_E solutions (concentrated, $A_{195}=2$ and diluted, $A_{195}=0.8$) was measured for a range of pH values. While there was no absorbance peak observed in the middle pH range (pH 4-9) for DI water, a prominent UV absorbance was registered for I_E water in the same pH range (Figure 15). The strong UV absorbance peaks were noted for all solutions under extreme acidic (pH<4) or basic (pH>9.5) environment, which can be explained by the dominating effect of monopoles in those areas.

The resistivity of two types of I_E solutions, called Y-R and C-R, was analyzed as a function of their relative concentrations, based on UV absorbance at $\lambda =195$ nm (Figure 16). The I_E solution of higher concentration had lower resistivity.

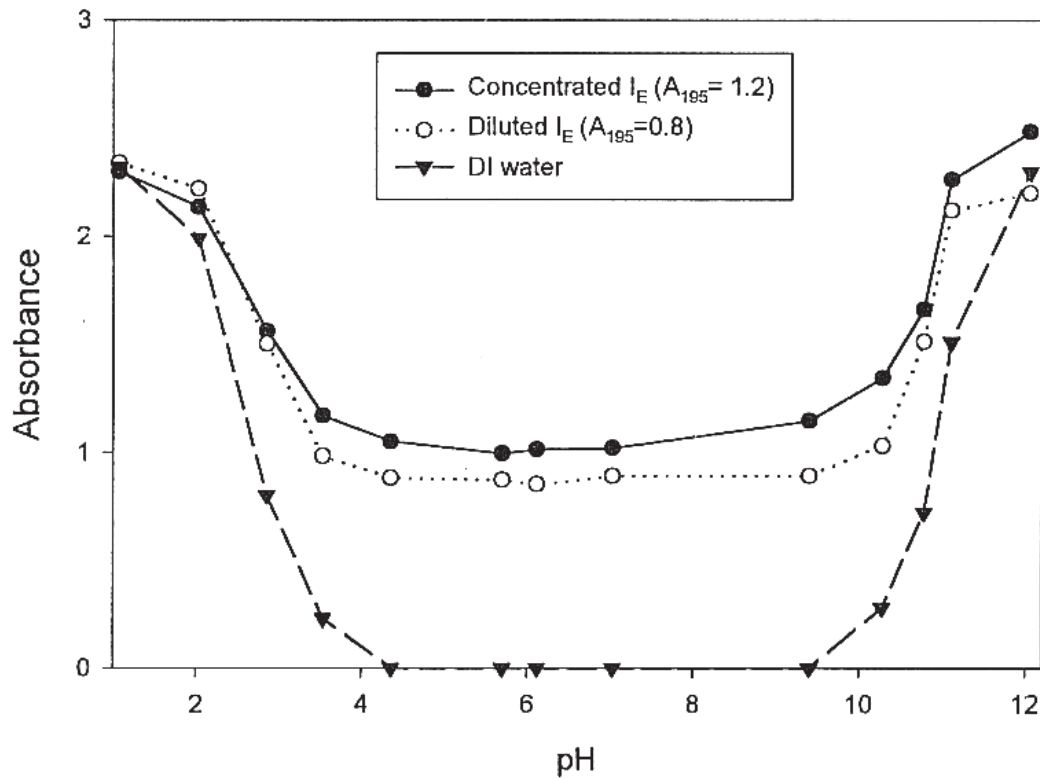


Figure 15 The UV absorbance at $\lambda=195$ nm versus pH value for two different concentrations of and I_E solution, and DI water.

The resistivity of these two I_E solutions differed by more than a factor of 2, indicating difference in their mobilities, perhaps due to different shapes of the I_E clusters. Resistivity measurements may provide a way to distinguish different kinds of I_E solutions. Another interesting feature was the large value of resistivity compared with that of an ionic solution. For one mole of NaCl solution, the resistivity, was about $32\Omega\text{-cm}$. The resistivity measured for the I_E solution, which is dipole solution, was 10,000 times smaller than that for the monopole ionic solution.

5 A Discussion on Contaminants

The crucial question in interpreting the above data is whether the results are artifacts. I_E samples were prepared in a clean room using water purified by deionization (Millipore Ultrapure System, San Francisco, CA), and contained less than 10 ppb of total dissolved solids. However, pure water is known to be very reactive, and its purity rapidly decreases when it is exposed to air. The resistivity of water processed by the Millipore Ultrapure System is 18.2 $M\Omega/cm$, but as soon as the water exits the system, the resistivity drops to 6 $M\Omega/cm$, then to 2 $M\Omega/cm$ and slowly drifts down to 1 $M\Omega/cm$. The phenomenon is due to absorption by water of various contaminants and CO_2 , from the air. Dissolved in water, CO_2 forms, carbonic acid, which together with other dissolved impurities from the air contributes to an increase in the number of ionic species in water, which in turn causes a decrease in resistivity and an increase in conductivity of water.

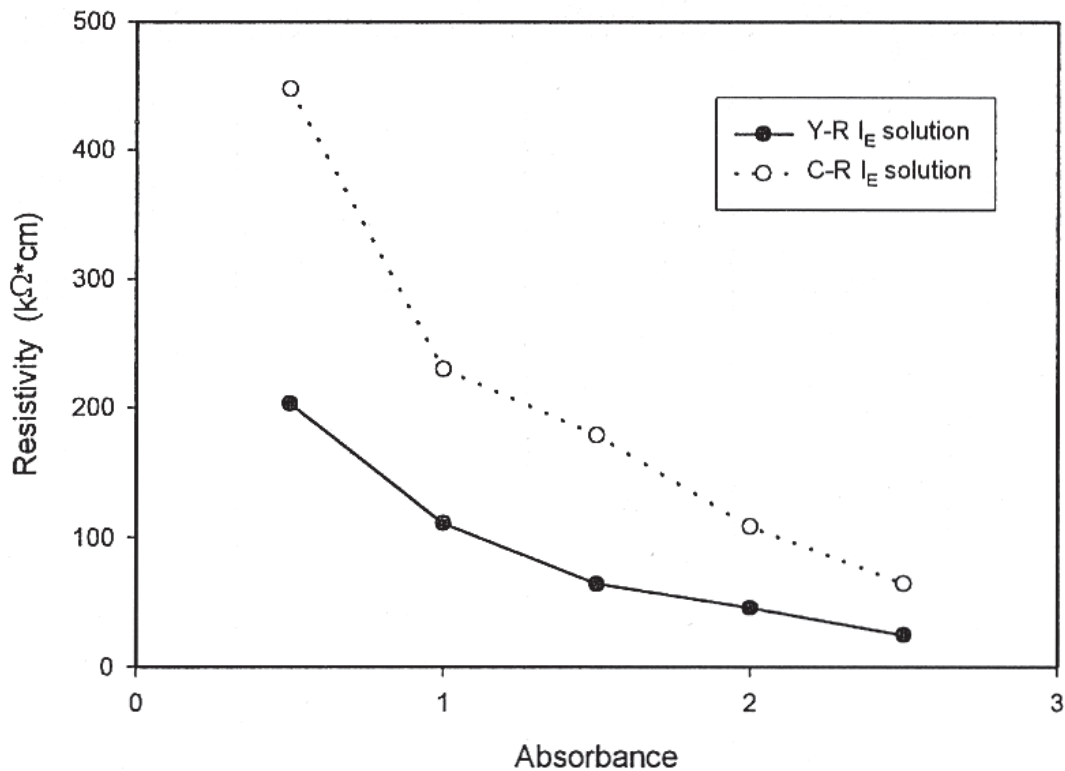


Figure 6 The resistivity of I_E water vs. its relative concentration as indicated by UV absorbance at 195nm.

All reported results were obtained with DI water as a control. Typically, the measured parameters for I_E aqueous solutions were 4 orders of magnitude higher than the background. Therefore, the contribution of impurities from the water used for I_E solutions' preparations to the measured physical and chemical properties of I_E can be ruled out. Prior research results³⁷ established that there is about a 20% decrease in dielectric constant for a I_E water at 10⁶ Hz, as compared with ordinary water.

Contaminants can be broadly classified into inorganic and organic. "Polywated" was claimed to have been discovered in the '60s and '70s, but later its anomalous properties were attributed to a silicon impurity. To distinguish I_E water from polywater, two classes of inorganic contaminants were considered: ionic and silicon. The organic contaminants were separated into two groups: volatile, which have a boiling point above that of water, and nonvolatile, with a boiling point below that of water (Table 4).

UV absorbance analysis of I_E solutions before and after distillation demonstrated that the characteristic UV signature of I_E solutions is not due to impurities. I_E clusters, composed of water molecules, evaporated and condensed together with ordinal' water in a distiller, leaving non-volatile impurities behind.

	Inorganic		Organic		Biological
	Ions	Silicon	Volatile T _{b.p.} >100°C	Non-volatile T _{b.p.} >100°C	Micro- organism
1. Distillation					
(1.a) UV absorbance of double distilled I _E water.	x	x	✓	x	x
(1.b) Residues from evaporation.	ppm	ppm	✓	ppm	ppm
2. Images					
(2.a) TEM (x-ray)	x	x	x	x	✓
(2.b) AFM	—	—	—	—	x
(2.c) Laser autocorrelation	—	—	—	—	x
3. Electrical properties ³⁷					
(3.a) Conductivity	x	x	x	x	x
(3.b) Dielectric constant	x	x	x	x	x
(3.c) Emf	x	x	x	x	x
4. Physical properties ³⁶					
(4.a) Density	10 ppm	10 ppm	10 ppm	10 ppm	10 ppm
(4.b) Boiling point	x	x	x	x	x
5. Electromagnetic response ³⁷					
(5.a) UV fluorescence		x			
(5.b) IR	x	x	✓	✓	x
(5.c) Low frequency AC	x	x	x	x	x

x -- an effect of contamination can be ruled out, ✓ -- an effect of contamination cannot be ruled out

A concentrated I_E solution was distilled twice. Samples of the original solution, the first and the second distillates were analyzed with a Perkin-Elmer UV/Vis Lambda 2S spectrophotometer (Norwalk, CT) within 190-300 nm wavelength range (Figure 17). The maximum UV absorbance of I_E solution remained the same after the first and the second distillation. There was a small change in UV absorbance observed after the first distillation, but hardly any change in the UV absorbance occurred after the second distillation. The UV signature, with a peak around 195 nm and a shoulder between 200 - 210 nm observed in I_E solution prior to and after distillation, could not come from any non-volatile contaminants. Therefore, inorganic and non-volatile organic contaminants, as well as microorganisms can be ruled out as sources of the UV absorbance in the discussed region. This experiment, however, did not rule out a possibility of contamination by volatile organic substances.

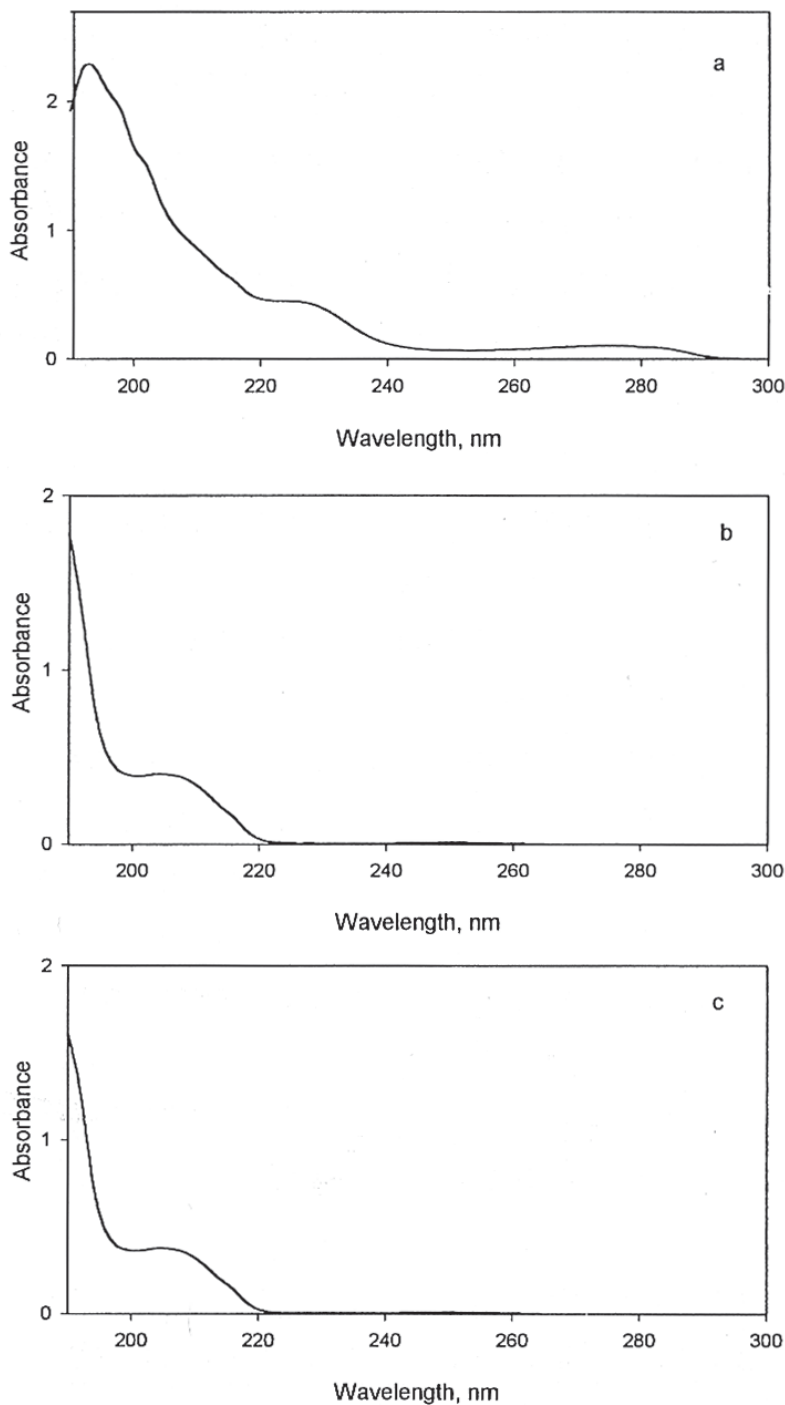


Figure 17 UV absorbance vs. wavelength for I_E water (a) before distillation, (b) after the first distillation, (c) after the second distillation.

I_E Crystal samples for TEM analysis were prepared by depositing the I_E solution on filter paper, coating it with carbon, and then boiling in chloroform for twenty minutes. This process removed all volatile organic contaminants from I_E samples, and therefore the structures identified on TEM images cannot be attributed to the presence of volatile organic contaminants.

The analysis of x-ray spectra obtained by focusing the electron beam on any I_E cluster ruled out inorganic contaminants.

Even though single I_E structures do look like bacteria containing gas vesicles, the clusters that they form are too regular in shape to be described as microorganisms. Moreover, TEM of sterilized by boiling I_E solutions still revealed I_E clusters. It is highly unlikely, therefore, that the structures observed in TEM photographs are of microbial nature. The combined results of the distillation experiments and TEM analysis ruled out any conceivable contaminants above ppm level (Table 4).

Some of the properties of I_E solutions discussed in this paper present strong evidence against various contaminants and their effect on properties of I_E clusters:

- a) Inorganic ions: As discussed in section 4, ions are monopoles. Monopole-monopole and monopole-dipole types of interaction can not account for electrical properties of I_E solutions.
- b) Silicon: The x-ray spectra, recorded by focusing an electron beam on an I_E cluster detected with TEM, rule out silicon as a source of I_E Crystals. Silicon, however, was identified as a component of particles found in control water samples.
- c) Volatile Organics: The method of I_E sample preparation for TEM analysis described above eliminates a possibility that the detected structures are due to volatile organics.
- d) Nonvolatile organics: The UV absorbance measurement of distilled I_E solution rules out this type of contamination.
- e) Microbial contamination: Microorganisms cannot contribute to the electrical properties of I_E solutions. Since microorganisms can be effectively removed by distillation, UV absorbance data of distilled I_E solutions indicate other than microbial origin of I_E clusters. Additionally, the morphology of I_E clusters viewed with AFM and results of laser autocorrelation experiments support this conclusion.

Industrial application of I_E water does not require ultra purity of I_E solutions, The presence of contaminants at ppm levels is acceptable, when a significant favorable effect is achieved in physical, chemical, or biological systems. Additional research is required to establish existence of I_E clusters without an initiator. Our main goal at this time, however, is to further improve the beneficial effects of I_E clusters in a wide range of applications.

6 Applications

Since I_E clusters are made of water molecules, almost unlimited possibilities for I_E clusters applications exist in the areas where ordinary water can be substituted with I_E water. Only a few potential I_E water applications have been investigated so far:

Application Area	Testing Area
Physical Processes	<ul style="list-style-type: none">• Descaling• Cleaning
Chemical Processes	<ul style="list-style-type: none">• Enhancement of combustion• Reduction of coke formation in ethylene production
Biotechnology	<ul style="list-style-type: none">• Regulation of enzymatic activities and microbial growth
Medical	<ul style="list-style-type: none">• Stimulation of immune responses to infection and cancer

6.1 Scaling Reduction and Cleaning Enhancement

It has been established by AFM and photon autocorrelation measurements that I_E clusters range from 10-20 nm to 1-5 μm in size (Section 3). Since smaller I_E clusters have larger electric dipole moments (Sections 4.2 and 4.3), it is necessary to break large I_E clusters into small ones. prior to an application, to achieve the maximum effect. A mechanical stirrer, a static mixer, or ultrasound can be used for this purpose.

Scaling of heat transfer equipment by calcium and magnesium carbonates is a common problem. Traditional chemical scale mitigation methods require higher running costs and produce a negative environmental impact. The use of the I_E water to eliminate seating is an attractive cost-efficient and environmentally friendly alternative. I_E clusters provide a center of nucleation for the calcium carbonate growth, which prevents scale deposition on the walls of heat transfer equipment (Figure 18).

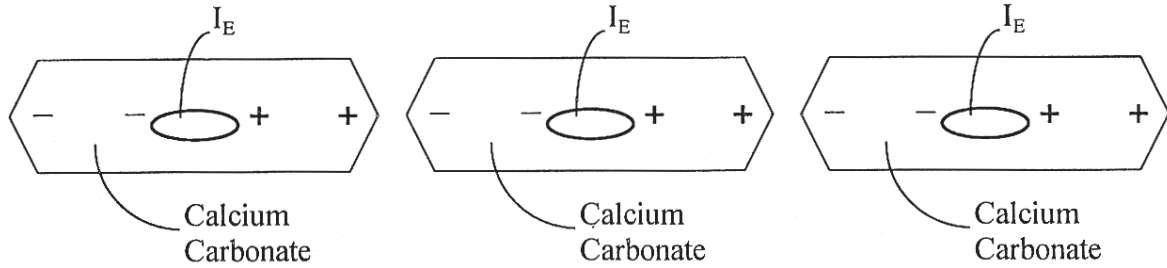
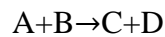


Figure 18 Effect of descaling by I_E clusters. Due to the strong electric field, calcium carbonate will nucleate around the I_E Crystals and not deposit on the wall.

The effect of I_E clusters on surface tension is being studied by several research groups. The sonication of I_E water has been observed to result in reduction of solution's surface tension. In a traditional cleaning or washing process, soils are removed from a surface by surface active substances (surfactants). I_E clusters may enhance detergency due to electrostatic attraction between the electric dipole moment of the I_E clusters and the induced electric dipole moment of the soil, assuming the soil is made up of dielectric materials. Although, further in depth research is required, a potential for use of IE water in commercial cleaning applications does exist.

6.2 Enhancement of Chemical Reactions

Current research indicates that I_E solutions enhance the oxidation of hydrocarbon, carbon, and carbon monoxide. These observations can be attributed to the effect of electric dipole moments of I_E clusters in chemical reactions. Let us consider a very simple reaction in which A reacts with B to give products C and D:



The reaction rate (R) of this reaction can be written as:

$$R = n_A n_B v_{AB} \sigma (AB \rightarrow CD), \quad (10)$$

where n_A n_B are the densities of A and B, v_{AB} is the relative velocity of A with respect to B, and $\sigma (AB \rightarrow CD)$ is a cross section of the reaction. The electric dipole moment of the I_E clusters can influence this reaction rate in two ways.

The densities n_A and n_B will be increased in the proximity of IE clusters. Assuming that the chemical species are in equilibrium in a gaseous state, the distribution of chemicals n_A and n_B obey Boltzman distribution:

$$\begin{array}{l} n_A = \exp(-\phi/kT) \\ n_B = \exp(-\phi/kT), \end{array} \quad (11)$$

where ϕ is an electric potential exerted by the permanent electric dipole moment D of the I_E clusters onto A and B. The electric field emitted by I_E clusters will induce an electric dipole in A or B, which will be then attracted to the I_E clusters. The value of electric potential ϕ depends on the distance (r) between an I_E cluster and a molecule A (or B):

The closer a molecule to an I_E cluster, the larger the potential ϕ , the Boltzmann factor, and as a result the density n_A (or n_B) is higher (Figure 19).

$$\phi \sim 1/r^3 \quad (12)$$

Additionally, a molecule A (or B) will be attracted by electric dipole force towards the I_E clusters, which will result in higher relative velocity v_{AB} . A and B molecules will move faster around I_E clusters which will lead to a higher reaction rate.

Should the above hypothesis be true, then the catalytic effect of I_E Crystals is a volume rather than a surface phenomenon, which separates I_E clusters from such well-known catalysts as platinum. If the enhancement of the chemical reaction occurs mostly near the I_E clusters, then the particular surface or charge distribution of an I_E cluster is not critical. The only relevant factor is the net electric dipole moment of that particular I_E cluster.

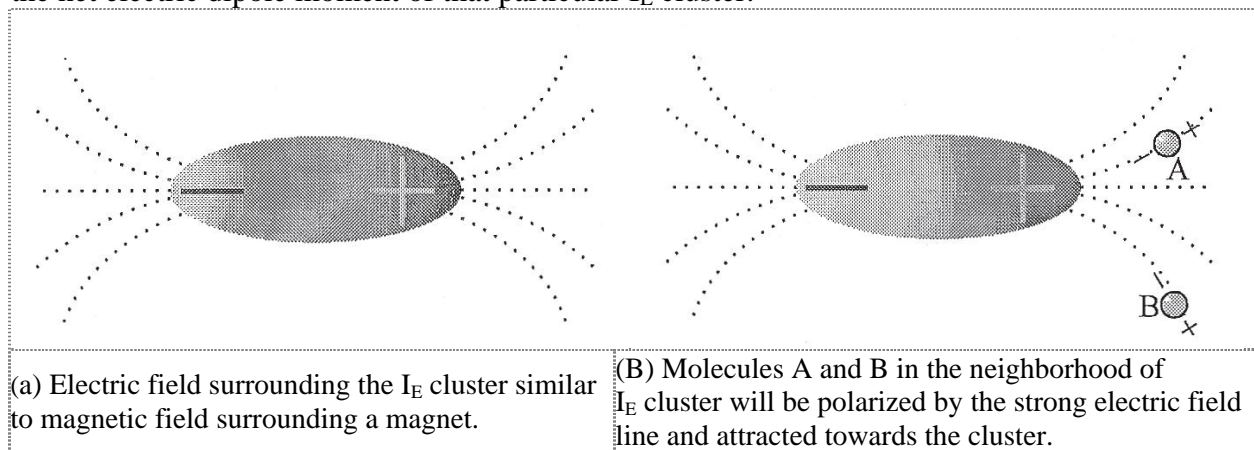
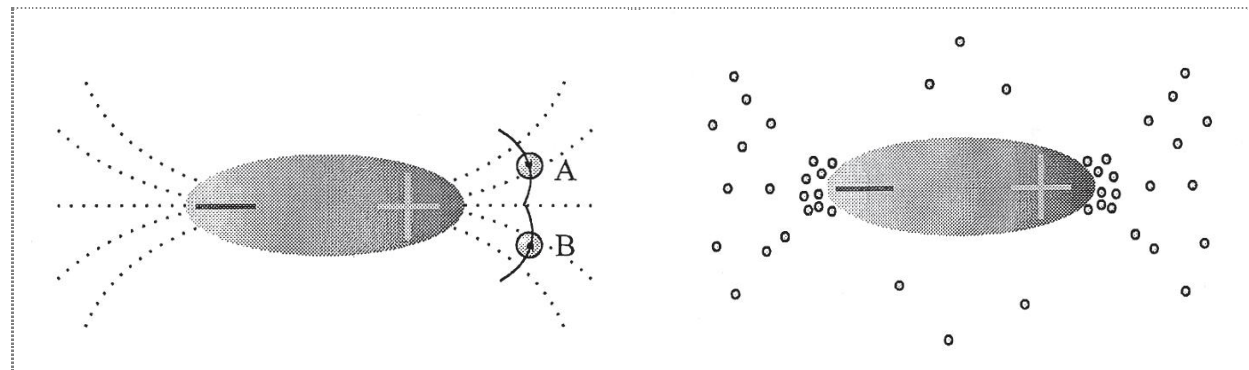


Figure 19 Enhancement of a chemical reaction by an I_E cluster.



(c) When A and B collides, the relative velocity of collision is much larger than where there is no electric field from I_E .

(d) Due to strong electric field near the positive and negative pole of I_E clusters, the densities of molecules A and B are much higher than places where there is no electric field.

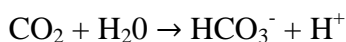
Figure 19 (cont.) Enhancement of a chemical reaction by an I_E cluster.

6.3 Influence of I_E Clusters on the Activities of Enzymes

Enzymes, catalytic proteins, are known to enhance the rate of chemical reactions in biological systems by many orders of magnitude. Although, the mechanisms of a wide range of enzymatic reactions are under extensive investigation, scientists still cannot predict an enzymatic mechanism based on the known structure of an enzyme. Therefore, it is premature to make any definite conclusions about a mechanism behind the stimulating affect of I_E clusters on certain enzymes.

The following discussion is an attempt to propose a possible mechanism for I_E -enzyme interaction based on the known physical properties of I_E clusters. I_E clusters can form around a protein. Shaking of the protein solution will remove some I_E clusters from the protein, leaving some parts of I_E clusters intact. Further dilution and shaking of the protein solution may generate a negative-like image of the created water clusters, a template of a portion of the protein surface with similar charge density distribution. The obtained I_E clusters may act as catalysts, similar to the original enzyme. It is also conceivable that some I_E clusters may be attracted to the enzyme in a way that impairs its function as a catalyst, thereby reducing its activity.

The discussed hypothesis can be applied to the following simple enzymatic catalysis; the hydration of carbon dioxide by carbonic anhydrase:



The zinc ion plays a key role in the catalysis. Water bound to the zinc ion is converted into a hydroxide ion, which creates a high local concentration of OH^- . Zinc also helps orient the CO_2 , so it is positioned better for reaction with OH^- .

It is expected that an I_E solution, prepared with carbonic anhydrase as a seed material, will contain some I_E clusters which resemble zinc ion in surface charge density. Such I_E clusters might bind water and CO_2 similar to zinc ion, and therefore will catalyze the enzymatic reaction.

It is also possible that some I_E clusters might be attracted to the zinc ion of the carbonic anhydrase and block its function as a catalyst. In this case, the addition of an I_E solution may suppress or even inhibit the enzymatic activity.

It is possible, therefore, to both stimulate and suppress enzymatic reactions, by optimizing the type of I_E solution used in a particular application.

6.4 Medical Application

The human body, which is approximately 70% water by weight, is an extremely complicated biological system. Based on the various properties of I_E clusters and some anecdotal evidence, we can speculate relative to four areas of medical applications.

6.4.1 Shape and Charge Density of I_E Cluster

I_E clusters may act as templates of the material used to induce their formation (seed). Therefore, I_E clusters may act as a harmless antigen that stimulates the production of antibodies and enhances the immune response to an infection or cancer.

6.4.2 Effect of Ultra Low Dosage

I_E clusters exist even when the concentration of the seed material is diluted down to below 10^{-7} mole. The I_E clusters can then regenerate themselves in further dilutions. Although the concentration of the seed becomes very small (on the order of ppb), the percentage of I_E clusters is quite large in the solution. The cell membrane is an osmotic membrane and can locally create a small amount of very pure water which is required for formation of I_E clusters. Many I_E clusters can be then generated by a cell from a single seed molecule. Therefore, a single seed molecule can influence many cells through formation of high concentrations of I_E clusters. The above hypothesis can be a basis for an explanation of efficacy of ultra low dosages (homeopathic remedies in particular) on human functions.

6.4.3 Electric Properties of I_E Clusters

The I_E clusters can generate electric potential up to 100mV. The existence of I_E clusters may be the underlying physical basis for the observed increase or a decrease of electric potentials in acupuncture points, as well as the meridian theory of acupuncture in general.

6.4.4 Electromagnetic Waves (em)

Electromagnetic waves are widely used in medical applications. A very short electromagnetic wave, such as a gamma ray, is used to treat brain cancer. The radio frequency em wave is used in magnetic resonance imaging. I_E clusters absorb UV energy at 195nm, and demonstrate a fluorescence emission at 295nm. These characteristics may be useful as diagnostic tools. The three peaks of low frequency em wave at kHz can also be used in the future for diagnostic purposes or as treatment.

7 Acknowledgments

Many of the results reported here are obtained from collaborations with Dr. Wen-Chang Li, Dr. Cheuk-Yin Wang and Dr. Olga Berson.

8 References

1. J.H. Jensen, and M.S. Gordon, *J. PHYS. Chem.* 99, 8091 (1995).
2. L.S. Sremaniak, L. Perera, and M.L. Berkowitz, *J. Phys. Chem.* 100, 1350 (1996).
3. C. Lee, H. Chen, and G. Fitzgerald, *J. Chem. Phys.* 102, 1266 (1995).
4. I.P. Buffey, W. Byers-Brown, and H.A. Gebbie, *Chem. Phys. Lett.* 148, 281 (1988).
5. C.J. Tsai, and K.D. Jordan, *Chem. Phys. Lett.* 213, 181 (1993).
6. C.J. Tsai, and K.D. Jordan, *J. Phys. Chem.* 97, 5208 (1993).
7. K. Liu, M.G. Brown, J.D. Cruzan, and R.J. Saykally, *Science* 271, 62 (1996).
8. C.J. Grueloh, J.R. Carney, C.A. Arrington, T.S. Zurci, S.Y. Frederieks, and K.D. Jordan, *Science* 276, 1678 (1997).
9. A. Vegiri, and S.C. Farantos, *J. Chem. Phys.* 98, 4059 (1993).
10. S.S. Xantheas, *J. Phys. Chem.* 100, 9703-9713 (1996).
11. S.S. Xantheas, and T.H. Dunning, Jr., *J. Chem. Phys.* 99, 8774 (1993).
12. S.S. Xantheas, *J. Chemt Phys.* 100, 7523 (1994).
13. K.S. Kim, M. Dupuis, G.C. Lie, and E. Clementi, *Chem. Phys. Lett.* 131,451 (1996).
14. A. Khan, *Chem. Phys. Lett.* 258, 574 (1996).
15. A. Khan, *Chem. Phys. Lett.* 253, 299 (1996).
16. J. Smets, W.J. McCarthy, and L. Adamowicz, *Chem. Phys. Lett.* 256, 360 (1996)
17. H. Sekiya, H. Hamabe, H. Ujita, N. Nakano, and Y. Nishimura, *Chem. Phys. Lett.* 255, 437 (1996)
18. M. Armbruster, *Phys. Rev. Lett.* 47(5), 323 (1981).
19. G. Nemethy and H.A. Scheraga, *J. Chem. Phys.* 36, 3382 (1962).
20. S.W. Benson, *J. Amer Chem. Sot.* 100, 5640 (1978).
21. K. Liu, J.D. Cruzan, and R.J. Saykally, *Science* 271,929 (1996).
22. N. Fletcher, *The Chemical Physic of Ice*, (Cambridge University Press, 1970).
23. S. Dong, A.I. Kolesnikov, and J.C. Lo, *J. Phys. Chem. B*:101, 6087 (1997).
24. S.M. Jackson, V.M. Nield, R.W. Whitworth, M. Ogriro, and C.C. Wilson, *J. Phys. Chem. B*, 101, 6142 (1997).
25. I. Morrison, J.C. Li, S. Jenkins, S.S. Xantheas, and M.C. Payne, *J. Phys. Chem. B*, 101, 6146 (1997).
26. C.A. Tulk, H. Kiefte, M.J. Clenter. and R.E. Gagnon, *J. Phys. Chem. B*, I01, 6154 (1997).
27. S.M. Jackson, and R.W. Whitworth, *J. Phys. Chem. B*, 101, 6177 (1997).
28. I.M. Svishchev, and P.G. Kusalik, *Phys. Rev. Lett.* 73,975 (1994).
29. V.P. Dimitriev, S.B. Rochal, and P. Toledano, *Phys. Rev. Lett.* 71,553 (1993).
30. M. Garfish, R. Poporitz-Biro, M. Lahav, and M. Leisterowicz, *Science* 250, 973 (1990).
31. *Proceedings of the International 5;ymposium on the Physics and Chemistry of Ice*, eds. N. Maeno, and T. Hondoh (Hokkaido University Press, Sapporo, Japan 1992).
32. *Seventh Symposium on the Physics and Chemistry of Ice*, J.Phys. Chem. 48, Colloq. No. 1

Supplement, Fasc. 3, XV, 707 (1987).

33. *Sixth Symposium on the Physics and Chemistry of Ice*, J. Phys. Chem. 87, 4015, 340 (1983).

34. *Symposium on the Physics and Chemistry of Ice*, J. Glaciol, 21, 714 (1977).

35. W. Stumm and J.J. Morgan *Aquatic Chemistry. An Introduction Emphasizing Chemical Equilibria in Natural Waters* (John Wiley & Sons, New York 1981).

36. S.Y. Lo, *Modern Phys. Lett. B*, 10, 909 (1996).

37. Shui Yin Lo, Angela Lo, Li Wen Chong, Lin Tianzhang, Li Hui Hua, and Xu Geng, *Modern Phys. Lett. B*, 10,921 (1996).

38. There are a great deal of work on water clusters existing in isolation see examples from NATO Advanced Institute Recent Theoretical and Experimental Advances in Hydrogen-Bonded Clusters, 22, June 4, July 1997, EIounda, Crete, Greece, edited by S.S. Xantheas, to be published as a book. The water clusters discussed here are formed in water not in isolation.

39. C.Y. Wong and S.Y.Lo in *The Proceedings of The First International ,Symposium on the Current Status of the IE Crystal Technology*, (World Scientific, 1998).

40 S. Magonov in *The Proceedings of The First International Symposium on the Current ,Status of the IE Crystal Teehnolog3*, (World Scientific, 1998).